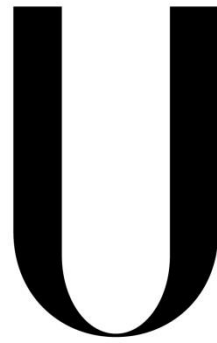


**UNIVERSIDADE DE LISBOA**

**FACULDADE DE CIÊNCIAS**

*DEPARTAMENTO DE BIOLOGIA ANIMAL*



**LISBOA**

---

UNIVERSIDADE  
DE LISBOA

**Somitogenesis and Fibronectin:  
United by tension?**

Gonçalo Goulart da Silva Pinheiro

DISSERTAÇÃO

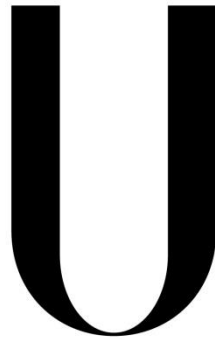
MESTRADO EM BIOLOGIA EVOLUTIVA E DO DESENVOLVIMENTO

2014

**UNIVERSIDADE DE LISBOA**

**FACULDADE DE CIÊNCIAS**

*DEPARTAMENTO DE BIOLOGIA ANIMAL*



**LISBOA**

---

UNIVERSIDADE  
DE LISBOA

# **Somitogenesis and Fibronectin: United by tension?**

**Dissertação de Mestrado orientada por:**

Prof. Doutora Sólveig Thorsteinsdóttir

Gonçalo Goulart da Silva Pinheiro

DISSERTAÇÃO

MESTRADO EM BIOLOGIA EVOLUTIVA E DO DESENVOLVIMENTO

2014



# Contents

Acknowledgments .....	2
Resumo .....	3
Abstract .....	6
Introduction.....	7
Materials and Methods .....	15
Embryo Development.....	15
Experimentation .....	15
Explant cultures .....	15
<i>In Situ</i> Hybridization .....	16
Immunolabelling.....	17
Image Acquisition and Treatment .....	19
Stereoscope Microscopy .....	19
Confocal Microscopy .....	19
Results .....	20
Expression pattern of <i>fn1</i> and <i>itga5</i> , key genes involved in FN matrix assembly.....	20
FN matrix assembly and development.....	24
Culturing with RockOut, a cellular tension-reducing drug .....	26
Effects of loss of tension in somite formation, maturation, and matrix assembly .....	26
Effects of loss of tension on gene expression during somitogenesis.....	33
Discussion .....	41
The Development of Matrix Assembly .....	41
The complicated relationship between tension and matrix .....	43
Does tension affect patterning? .....	44
Bibliography.....	46

# Acknowledgments

# Resumo

A somitogénese é um processo conservado em vertebrados, responsável pela determinação da segmentação do sistema musculo-esquelético que permitiu a adaptação dos métodos de locomoção aquática a ambientes terrestres. A extrema importância do correcto desenvolvimento deste processo para a formação do embrião fez com que a rede regulatória responsável por coordenar este processo tivesse evoluído para uma das mais complexas observáveis no embrião. Todos os dias novos intervenientes neste processo são descobertos, tornando-se cada vez mais óbvio que este é de facto um processo altamente complexo e robusto, garantindo vias alternativas de regulação em caso de falhas no sistema.

Para tentar explicar, de uma forma simplificada e teórica, o modo de regulação do processo de somitogénese, no século passado vários modelos foram propostos. Hoje em dia o modelo mais aceite é o de “Clock and Wavefront”. Este modelo, proposto em 1976 por Cooke and Zeeman, supoe a existência de uma interacção de factores, cuja produção é cíclica, que marca o “tempo” que as células passam numa zona indeterminada da mesoderme paraxial. Associada a esta ciclicidade de factores encontra-se-ia um gradiente de um outro factor, distinto dos primeiros, que seria responsável por determinar a maturidade das células. Quando células que já passaram por um certo número de ciclos atingem uma determinada região do gradiente, estas interpretariam a combinação de ambos os sinais como informação para se diferenciarem e aglomerarem, formando um novo sómito.

Desde a proposta deste modelo, vários genes foram descobertos que suportam este processo de regulação da somitogénese. Estes foram associados ao “relógio” molecular, quer como fazendo parte, quer como sendo regulados por ele, contando-se entre eles os genes *hairy/hes*, *meso/mesp* e *lunatic fringe*, e os genes aparentemente responsáveis pela determinação do gradiente caudal foram identificados, sendo eles *raldh* (responsável pela transformação de retinaldeído em ácido retinóico) e *fgf8*.

Para além destes genes muitos outros foram sugeridos como participantes no processo de somitogénese. Ephrinas, caderinas, integrinas, fibronectina, *sonic hedgehog* e WNT's foram associados ao processo de somitogénese uma vez que os mutantes para cada um dos genes, para além de outros defeitos, apresentam interrupção ou perturbação do processo de somitogénese.

De entre estes, um gene que suscitou bastante interesse foi o de Fa. Há muito que se sabe que a FNa é um componente da matriz extracelular importante para vários processos durante o desenvolvimento do embrião. Embriões mutantes para fibronectina apresentam incapacidade de formar sómitos. No entanto, o papel exacto da matriz de fibronectina neste processo mantém-se pouco claro. Certamente que em parte funcionará como suporte físico, mas um número crescente de estudos têm surgido que demonstram que a matriz extracelular não serve apenas de “andaime” para as células, mas contém de facto informações químicas e físicas muito importantes para os processos de morfogénese que ocorrem durante o desenvolvimento embrionário.

Dois destes estudos tiveram como foco do seu trabalho a própria fibronectina, e o seu papel na regulação do processo de somitogénese. Rifes et al. e Rifes e Thorsteinsdóttir, em 2007 e 2012, respectivamente, demonstraram que: (1) a fibronectina é expressa pela ectoderme e montada em redor da mesoderme presomítica, (2) que sem a ectoderme e matriz a somitogénese pára, (3) e que a matriz existe num gradiente decrescente de complexidade, de anterior para posterior, levando à proposta de que o gradiente poderia estar a criar um gradiente de sinalização física, participante provável na regulação da somitogénese.

Neste trabalho propusémo-nos em testar esta hipótese, focando-nos em particular no efeito que a perda de sinalização física (i.e. tensão) celular tem na matriz e no processo da somitogénese, e por sua vez que efeitos tem a disrupção da matriz na regulação da somitogénese.

Começámos por realizar hibridações *in situ* para os genes *fn1* e *itga5* (respectivamente o gene que codifica para fibronectina em galinha e o gene que codifica o seu principal receptor na mesoderme paraxial) nos primeiros 12 estádios de desenvolvimento embrionário da galinha, *in ovo*, e a fazer imunomarcagem para a proteína de fibronectina. Observámos que o padrão de expressão destes genes se correlaciona intimamente com o padrão de montagem da matriz de fibronectina nos primeiros quatro estádios do desenvolvimento. Após esses 4 estádios a correlação contínua muito forte, mas começa a ser observável a existência de alguns tecidos que mostram montagem de matriz, mas não expressão do receptor, indicando a participação de outros receptores. É também observável o aparecimento de tecidos que expressam fibronectina, mas não o seu receptor, e tecidos que apenas expressam o receptor, mas onde existe montagem da matriz. Isto indica, como já tinha sido sugerido por Rifes et al., em 2007, que alguns tecidos produzem a matriz de FNa que outros irão montar, actuando esta como uma espécie de factor “parácrino”.

A seguir decidimos testar o efeito da perda de tensão na montagem *de novo* e manutenção da matriz e na morfologia dos sómitos, em explantes de embriões entre o estádio HH10 e HH13. Ao cultivar com RockOut, uma droga que inibe a fosforilação da Rho cinase III (ROCK), responsável pela estimulação da contracção da miosina não-muscular II, observámos um decréscimo acentuado da montagem da matriz de fibronectina, tanto após 6h de cultura como após 12h. Observámos também uma perturbação do processo de epitelialização dos sómitos, tanto nos sómitos formados antes como durante cultura, correlacionado com alterações na matriz de laminina. Enquanto que após 6h de cultura a epitelialização parece bastante afectada, a matriz de laminina encontra-se mais densa. Após 12h, quando a epitelialização parece já ter recuperado, tendo um aspecto mais normal, a densidade da matriz de laminina também se aparenta mais com a observada nos explantes controlo. Isto sugere que a matriz de FNa é importante para a epitelialização dos sómitos, mas caso esta se apresente perturbada a matriz de laminina tem a capacidade de compensar por ela, permitindo uma epitelialização correcta, ainda que com um atraso de pelo menos 6 horas.

Por fim decidimos analisar de que modo alguns genes, conhecidos por fazerem parte da regulação da somitogénese, são afectados pela perda de tensão. Para isso procedemos à cultura de explantes bissectados, nos quais as estruturas axiais foram divididas equitativamente por ambas as metades, de modo a cultivarmos cada metade num meio diferente, servindo uma de controlo à outra.

Este método permitiu-nos observar que a expressão dos genes responsáveis pela montagem da matriz de fibronectina não é afectada pela falta de tensão, mas que a expressão dos genes responsáveis pela frente de determinação da mesoderme pré-somítica sofre um ligeiro avanço rostral e que os genes de expressão cíclica, *hairy1* e *meso1*, apresentam um atraso na sua expressão. Estes resultados sugerem um atraso geral nos mecanismos celulares, tanto na maturação celular como na formação de novos sómitos.

Todos juntos, estes resultados indicam que a tensão celular é importante para o correcto estabelecimento da matriz extracelular da mesoderme paraxial, que por sua vez é muito importante para a correcta e atempada epiteliação dos sómitos, inicialmente auxiliada pela matriz de fibronectina, mas que pode ser compensada mais tarde pela matriz de laminina.

**Palavras-chave:**

*Somitogénese, Fibronectina, Expressão, Matriz, Tensão*

# Abstract

Somitogenesis is the founding morphogenetic process to all the skeletomuscular components of the vertebrate body. To describe the regulation of this process, in 1976, Cooke and Zeeman postulated the “Clock and Wavefront” model. From then on several genes have been found to be responsible for the regulation of somitogenesis through the process suggested by Cooke and Zeeman. Hairy1, Hairy2, Lunatic Fringe, Meso1 and Notch have been, in chicken, associated with the “clock” part of the model, where Fgf8 and retinoic acid have been associated with the “wavefront” part. Besides this regulatory network, other genes have been found to influence somitogenesis, like Wnt family genes, Sonic Hedgehog, BMP's and others. One of these genes, Wnt3a, was proposed in 2004, by Schmidt et al., to be the gene that confers ectoderm its indispensable role in somitogenesis. In 2007 Rifes et al. proposed that the gene responsible for the ectoderm's essential role was FN. In this work the authors showed that the unavailability of both the ectoderm and the FN matrix led to an arrest of somite formation, while with one or the other this arrest would not happen. It was proposed that the FN matrix, produced by the ectoderm and assembled by the paraxial mesoderm, would be essential for somitogenesis, and its role is to confer the proper tension information to the presomitic mesoderm (PSM), which might be indispensable for the PSM's correct and timely maturation.

In this work we continue the exploration of this hypothesis. First we analyzed the expression patterns of *fn1* and *itga5* (the  $\alpha$  chain of the major FN receptor, the  $\alpha5\beta1$  integrin) and how they correlate with matrix assembly in the early embryo, from stage HH1 to HH12. Then we cultured explants in RockOut, a Rho kinase III inhibitor that leads to the disassembly of non-muscle myosin II (resulting in a loss of tension) and assessed the effects on morphology and matrix assembly. Finally, we produced bisected explants that were also cultured with RockOut to test for effects on the genetic regulation of somitogenesis. We conclude that loss of tension leads to a delay in somite formation and epithelialization, which is later compensated by an increase in laminin matrix deposition.

## Key words:

*Somitogenesis, Fibronectin, Expression, Matrix, Tension*

# Introduction

Evolutionarily, the appearance of a third embryonic cell layer was a major breakthrough in animal development. While diploblastic animals are rather simple and form few differentiated tissues, that act as “jack-of-all-trades”, where each tissue is responsible for several different functions and metabolisms, triploblastic animals exist in an immensity of forms, shapes and sizes, and inhabit almost all existing ecosystems on Earth. The separation of functions between different organs and tissues made it possible to exert selective pressures upon each individual tissue and its function, without interfering with other vital functions, allowing triploblastic embryos to adapt and exist in the most variable conditions<sup>1</sup>.

The third embryonic layer, mesoderm, forms during an embryonic process named gastrulation, which in amniote embryos (reptiles, mammals and birds) occurs in very similar ways. In all of them the blastula stage embryo is formed by a two-layered disc of cells, the epiblast and the hypoblast, and the cells of the epiblast converge to the center of the embryo to form the primitive streak, which establishes the Anterior-Posterior (A-P) (also denominated Rostro-Caudal, R-C) and Dorso-Ventral (D-V) axes, as well as determine left and right sides. This converging leads to the formation of a depression, the primitive groove, through which migrating cells pass into the deep layers of the embryo. In the most anterior region of the primitive streak a regional thickening of cells, the Hensen’s Node, forms when the primitive streak starts to expand anteriorly. Hensen’s Node forms a depression in its center through which cells can also migrate as it moves in a caudal direction along the A-P axis, allowing cells to migrate through it at all levels of the axis, maintaining a steady production of mesodermal cells even after Hensen’s Node reaches the most caudal region of the embryo, while the embryo is still elongating. At the end of gastrulation, mesodermal cells that migrated through the Hensen’s Node will have given rise to prechordal mesoderm, notochord and medial parts of the somites, while cells that migrated through the middle of the streak will have given rise to the lateral part of the somites, heart and kidneys, and the cells that migrated through the more posterior parts of the primitive streak will have given rise to lateral plate and extraembryonic mesoderm<sup>2,3,4</sup>.

Gastrulation is therefore the basis for the establishment of the paraxial mesoderm, a very important subset of the third embryonic layer, since this mesodermal region, which surrounds the axial structures, notochord and neural tube, will give rise to all the muscles and the axial skeleton of the vertebrate body, as well as axial tendons and articulations, blood vessels, dorsal dermis and brown fat cells<sup>5,6</sup>. Paraxial mesoderm can be divided into two different regions, a more anterior cephalic mesoderm, which will give rise to cephalic muscles, some connective tissue and sphenoidal and otic bones<sup>7,8</sup>, and a more posterior segmented mesoderm, which will give rise to the basoccipital bone of the cranium and all of the axial skeleton, tendons, blood vessels, dorsal dermis and brown fat cells as well as all the skeletal muscle of trunk and limbs.

The segmented mesoderm received its name due to the fact that it goes through a periodical segmentation process, from rostral to caudal, where metameric sphere-like structures, called somites, are formed. The periodicity of this process is, in normal conditions, very regular and species specific (although some species can have different periodicities along the A-P axis), and have very little intra-species variability in the total number of somites formed<sup>9</sup>.

Somites are transient aggregates of mesodermal cells that acquire a dynamic epithelial/mesenchymal state<sup>10</sup>. They are formed by a wave of epithelialization, from medial to caudal, then to anterior, and finally lateral, that transforms the cylindrical anterior presomitic mesoderm (PSM) into a sphere-like structure<sup>11,12,13,10</sup>, with the outside cells becoming elongated, and polarized with their apical side turned towards a central cavity, called the somitocoel, while some inner cells are present within the somitocoel (Fig. 1 A).

About 7 and a half hours after its formation in the chicken embryo the dorsal side of the somite continues to be a compact sheet of epithelial cells, the dermomyotome, while the ventral side has undergone an epithelial-to-mesenchymal transition (EMT), becoming the sclerotome (Fig. 1 B). The distinction between these two populations is of extreme importance because, even though there is extensive cross-talk between them, each one will give rise to very distinct tissues that will have intercalating dispositions in the embryo.

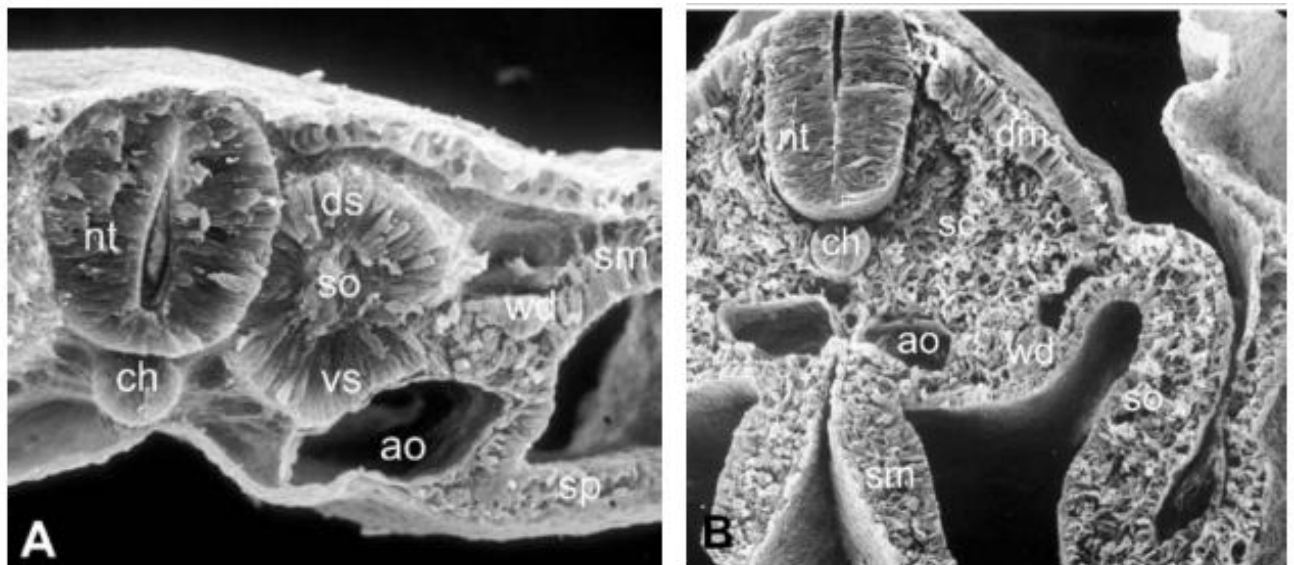
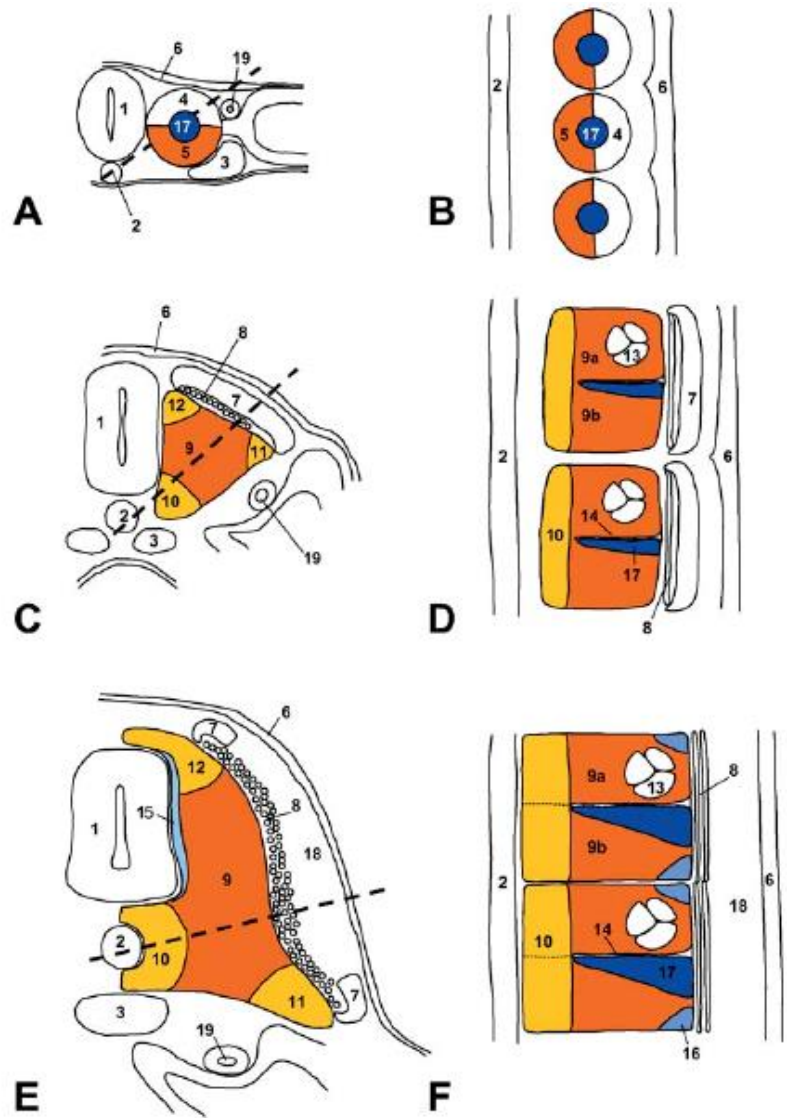


Figure 1- Scanning electron microscopic views on transverse fractures of a 2-day (A) and a 3-day (B) chick embryo showing the change in morphology of the somites between these two stages (ao aorta, ch notochord, dm dermomyotome, ds dorsal somite, nt neural tube, sc sclerotome, so somitocoele, sm somatopleure, sp splanchnopleure, vs ventral somite, wd Wolffian duct). Adapted from Christ et al., 2004.

The dermomyotome is a transient epithelial sheet formed from the dorsal somitic cells, which include the progenitors for all the muscles in the trunk and limbs, as well as dorsal dermis, among others<sup>6</sup>. It originates the myotome, which forms the scaffold upon which the deep back muscles (derived from the epaxial dermomyotome), as well as abdominal and intercostal muscles (derived from the hypaxial dermomyotome), will form. The formation of the myotome occurs through a progression of waves of cells coming from the dermomyotome. The first wave of cells comes from the dorsomedial lip and expands bidirectionally, both rostrally and caudally, forming the primary myotome. In the second wave the caudal, cranial, and finally ventrolateral,

border, in this order, also release myotomal precursors that will differentiate and enlarge the myotome. Finally, the central dermomyotome will deepithelialize, before the lips, and cells will both move dorsally to form the dermis, or parachute ventrally into the myotome, to add a third round of myogenic precursor cells. These processes will establish the embryonic “primitive” muscles, which show the ancestral segmentation pattern. Because this pattern is proper for aquatic locomotion, but not for life on land, the myotomes of reptilian, avian and mammalian embryos undergo a process called translocation, where the muscles realign to form the attachments appropriate for terrestrial locomotion. Besides the myotomal muscles, the hypaxial lip of the dermomyotome, at limb level, will also deepithelialize and migrate into the forming limbs, originating all the musculature found there, and at cervical level populations of cells also detach to migrate ventrally to give rise to the diaphragm or cranially to originate the tongue muscles.

The sclerotome is a mesenchymal bundle of cells, formed by the Pax1 expressing cells of the somitocoel and ventral somite, which will also start to express Pax9<sup>5</sup>. This region of the somite will then, through interactions with the axial structures and involving tissues, become regionalized, and in each region a population of distinct progenitors will arise. The sclerotome also forms a fissure between its rostral and caudal halves, called the von Ebner fissure<sup>14,15</sup>, which allows the caudal region of one sclerotome to fuse with the rostral region of the next one, in a process called resegmentation. This process is essential for vertebrate movements, because it allows the intercalation of muscles with the axial skeleton, important feature that can be seen in Osteichthyes, but also because it permits the migration of peripheral spinal nerves and initial blood vessels<sup>5</sup>. The regionalization of the sclerotome leads to the formation of distinct groups of progenitors which will give rise to tendon precursors, vertebrae, ribs and intervertebral discs, endothelial structures and meninges of the spine, intervertebral discs and joints of the vertebral column, and regulate the development of the DRG and spinal nerves. These regionalizations are depicted in Figure 2.



**Figure 2-(A-F)** Schematic representation of transverse and longitudinal sections of chick embryos at different developmental stages. **(A, B)** Epithelial somites. **(C, D)** Somites after compartmentalization. **(E, F)** Mature somites. Prospective sclerotome and sclerotome subdomains in color. The broken line in **A, C, E** indicates the section plane of **B, D, E** (1 neural tube, 2 notochord, 3 aorta, 4 dorsal half-somite, 5 ventral half-somite, 6 surface ectoderm, 7 dermomyotome, 8 myotome, 9 central sclerotome, 9a cranial half of central sclerotome, 9b caudal half of central sclerotome, 10 ventral sclerotome, 11 lateral sclerotome, 12 dorsal sclerotome, 13 spinal nerve, 14 von Ebner's fissure, 15 meningo-tome, 16 syndetome, 17 somitocoel cells/arthritis, 18 dermis, 19 Wolffian duct. Adapted from Christ et al., 2004.

Although both myotome and sclerotome go through complex morphological events (translocation and resegmentation, respectively) to bridge functionally, neither of these processes would be able to occur without the initial segmentation, established during somitogenesis. This must happen not only in the correct periodicity, but also in the correct direction, axial level and extension, because it is not only important that somites have a developmental difference of “n” minutes (species-specific) for proper resegmentation and muscle development to occur, but also that segmentation always happens first more rostrally, and progresses caudally in a gradual fashion, and that segments have the correct sizes, otherwise defects in the axial skeleton and muscle anchorage will occur.

Since so much depends on correct somitogenesis it is of no astonishment that this process must be highly regulated and robust. The model most accepted nowadays to represent the regulation of somitogenesis is the “Clock and Wavefront” model, proposed in 1976 by Cooke and Zeeman. They proposed that somitogenesis is regulated mainly by two factors, the first a “molecular clock”, that will establish the periodicity with which somites form based on the anabolic and catabolic dynamics of its constituents, in a repeating cycle. The second would be a

diffusible factor that exists in a gradient along the PSM, thus forming a “wavefront” (a certain concentration of that gradient) which moves posteriorly as the axis elongates. When the cells reach this wavefront, if they are in the correct cycle of the molecular clock, they will interpret the union of both signals as the signal to segment and epithelialize, forming a new somite.

From the proposal of this model researchers have tried to find a gene that would play one of the proposed roles by Cooke and Zeeman. In 1997 Palmeirim et al. found that *hairy1*, a chicken gene codifying a transcription factor downstream of the notch signaling pathway, shows a cyclic expression along the PSM, with a periodicity of 90 minutes (the same as somite formation) and its expression in the rostral PSM is concomitant with the formation of a new somite. From then on, several genes were found that fitted this model, like Notch1, Delta1 and 3, Lunatic Fringe, Hes/Hey/Her/Hairy family genes and Meso/Mesp family genes for the clock, and Fgf8, Fgfr1 and Raldh2 (enzyme responsible for the production of Retinoic Acid, RA) for the wavefront<sup>18-32</sup>.

Based on the expression patterns of these genes and how they interact with each other, it became apparent that the Notch signaling pathway is a major regulator of the “molecular clock’s” mechanism. As far as it is known now, it appears that Delta recognition activates Notch. Notch intracellular domain (NICD), which is produced when Notch is activated, is then translocated to the nucleus, where it induces the expression of Lunatic Fringe (*Infg*) and *hairy1*. *hairy1* will inhibit *Infg* and, when its expression levels get high enough, itself. *Infg* then modifies Notch’s activation by Delta, establishing this way the cycle of the “clock”. This cycle then signals boundary formation by inducing in the posterior “presumptive” s-l somite, through NICD, Meso1/Mesp2 expression, which will in turn induce expression of EphA4 in the rostral region of the presumptive s-l somite. EphA4 will bind to EphrinB2, present in the caudal region of s0, which will antagonize EphA4 and induce the formation of the cleft<sup>22,33-35</sup>. As for the gradient, RA inhibits Fgf8 expression anteriorly, limiting its rostral activity allowing the activation of the expression of Mesp/Meso, which in the posterior PSM is blocked by Fgf8 signalling through pERK<sup>36,37</sup>. A scheme of how the process might happen is represented in Figure 3.

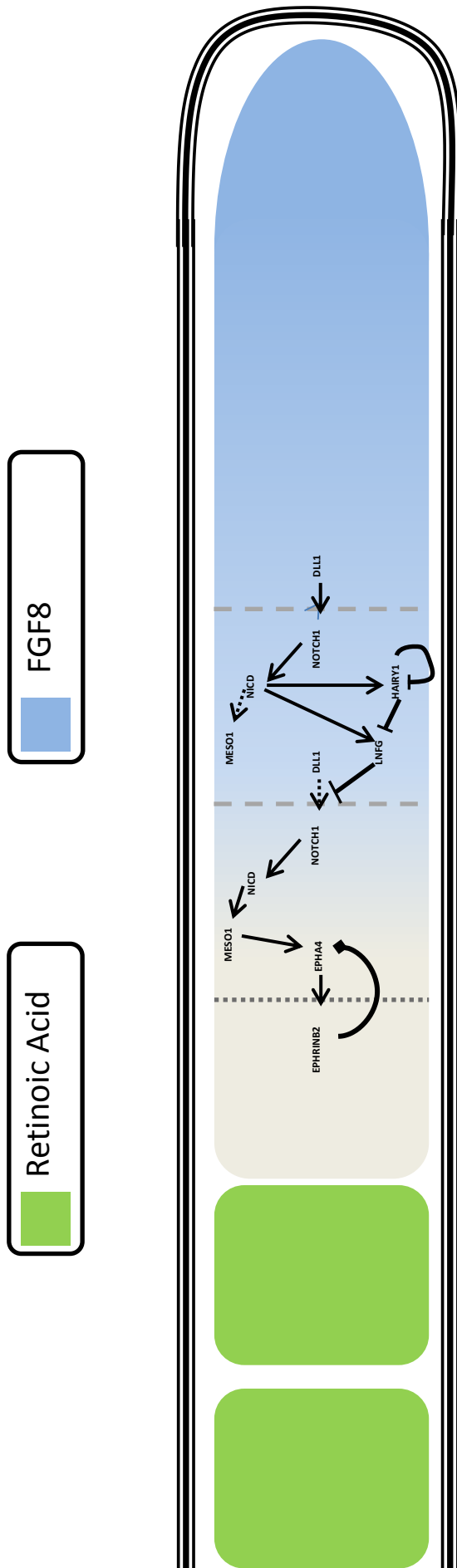


Figure 3 - Simplified schematic representation of the regulatory network of somitogenesis. The "molecular clock" is composed of the interactions between Notch, Delta, Hairy1 and Lunatic Fringe represented, which leads to cyclic expression and/or signaling through these pathways. The wavefront is established by confronting gradients of FGF8 and Retinoic Acid, which is expressed by the somites and inhibits FGF8, expressed in the PSM. A new somite is formed when, due to entering an area of the PSM with low enough levels of FGF8, cells can escape the repression of Meso1 expression. Meso1 will lead to the expression and interaction of Eph/Ephrin duos that will induce the formation of a cleft. Arrows indicate induction/activation. "Flathead" lines indicate repression/competition. "Diamondhead" lines indicate repulse.

Besides these genes, several others have been identified whose mutants show defects in somitogenesis and/or in the expression of the genes above, or whose expression is altered in mutants for the above genes. Some of the most studied include adhesion molecules like N-Cadherin<sup>38,10</sup>, essential for polarization and epithelialization of the somite, pFAK<sup>39</sup>, a phosphokinase involved in the signaling pathways of several adhesion molecules, transcription factors like Paraxis<sup>40-43</sup>, necessary for proper epithelialization of the somite, and Pax1, and Pax3 and Pax7<sup>44,6</sup>, responsible for determining dermomyotomal and sclerotomal lineages. Morphogens like Shh<sup>45-47</sup>, responsible for dorsal-ventral patterning of the somite, Noggin<sup>48</sup>, a BMP inhibitor necessary for paraxial mesoderm specification, and Wnt<sup>43,46,48-52</sup>, a group of genes that appear to have several functions, like gradient and clock establishment, regulation of epithelialization and participation in polarization, also have very important roles in somitogenesis. Although it was widely accepted that somitogenesis was a process independent of neighbouring tissues, some studies showed that even though the ectoderm is not necessary for molecular segmentation, it is required for physical segmentation<sup>53-55</sup>. Following these works it was initially proposed that the factor that confers ectoderm its importance was Wnt6, necessary for the correct polarization of the somites<sup>49,50</sup>.

In 2007, following several works on the topic of FN's role in somitogenesis<sup>38,53,56-62</sup>, Rifes et. al showed that the fibronectin (FN) matrix existent around the PSM is produced, in a rostral-to-caudal gradient, by the ectoderm, and to a lesser extent, endoderm, and then is assembled by the PSM, which expresses *Itga5*, the  $\alpha$  subunit of its assembly receptor,  $\alpha5\beta1$ <sup>63</sup>. They also showed that when this matrix is destroyed by enzymatic digestion somitogenesis is abolished, unless isolated PSMs are cultured with the ectoderm, or in a medium supplemented with FN. Furthermore, this matrix exhibits a gradient of increasing complexity, concomitant with the gradient of *fn1* expression in the ectoderm<sup>64</sup>.

These results suggest that FN is the ectodermal element necessary for somitogenesis to occur, and that this matrix protein might act like a "paracrine" factor. Since supplementing isolated PSMs with FN in the medium leads to a partial recovery of somitogenesis, it seems plausible that the matrix gradient established around the PSM could also create a gradient of physical signaling (i.e tension) that helps regulate somitogenesis.

It has been extensively demonstrated in other models, especially *in vitro*<sup>65-68</sup>, that tension, or physical cues, play important regulatory roles in several developmental processes, like cell migration and differentiation. Tension is as complex a characteristic to study as it is to characterize, since it is composed of so many levels and so many interactions with other regulatory systems. However, we can simplify it by looking at it at three distinct levels.

Tissue tension is the conjunction of pressures a tissue experiences from its neighbors as they undergo morphogenesis and change shape and size. At a smaller scale level there is matrix tension, which is defined by the density and rigidity of each individual component of the extracellular matrix (ECM), but also by the ability cells have to interact with each individual component, and then translate this physical information into chemical signaling (or internal physical signaling) that can then be dispersed through the cell, and to its neighbors. Finally, the lowest level is the one in which cells transmit the information to each other, and transform internal chemical and physical information into ECM alterations or cell-cell interaction alterations.

At this last level the effects of pathway signaling alterations and tension force alterations usually become hard to separate. This is due to the fact that it is at this level that the two merge, and inducing alterations in outside-in signaling leads mostly to the same defects as altering inside-out signaling. This makes it very hard, when studying tension, to determine whether or not tension is playing a role, or the effects induced are just from creating more system noise, like reducing cytoskeleton dynamics or generating ECM instability. However, since all of these are physical alterations, it becomes hard to say, even in those situations, that tension is not playing a part. In the end, tension bears some resemblances to a deity. Its existence and functions are hard to prove, but when you analyze all the effects your experiment produced, all could, in different degrees, be attributed to it. However, unlike a deity, you can remove it, and appreciate that it does have a clear effect, whether or not it is through influences in several systems.

Because it is hard to clarify their roles, how each level of tension regulates morphogenetic processes, and how they interact with each other, but there is a theoretical basis for the existence and functions of tension in somitogenesis, we decided to try and understand how it participates in the regulation of somitogenesis. To this end we cultured explants in the presence of a tension inhibiting drug, RockOut, and assessed how this affected (1) somite formation, (2) the morphological development of formed somites and PSM, (3) the deposition and assembly of FN and laminin (LN) matrix, two important components of the PSM and somite ECM and (4) the expression of genes implicated in somitogenesis, to try to understand how the first level of tension, the cellular level, interacts with the second level, ECM tension.

# Materials and Methods

## Embryo Development

Fertilized chicken (*Gallus gallus*) eggs were obtained from a commercial source (Sociedade Agrícola Quinta da Freiria, Portugal) and kept at 13°C until the desired incubation start time. Fertilized eggs were never kept for more than a week at 13°C. The eggs were incubated at 37°C ( $\pm 1^\circ\text{C}$ ) in a humidified atmosphere ( $\approx 70\%$  humidity) for the required amount of time necessary to obtain embryos at developmental stages ranging from HH1 to HH14 (Hamburger and Hamilton, 1951).

## Experimentation

### Explant cultures

Cultures of posterior embryo explants (PSM and last four somites) were performed, to be processed for mRNA expression and protein localization. Embryos used ranged from HH10 to HH14, since this is the period of development where forming somites are all thoracic somites (which have a different genetic regulation than the more rostral ones, Freitas et al., 2005; Rodrigues et al., 2006), the PSM has its longest length and surgical manipulation of axial structures is the easiest. Explants were recovered, staged and dissected in Complete Phosphate Buffer Solution (PBS, 137mM of NaCl, 2.68mM of KCl, 8.1mM of  $\text{Na}_2\text{HPO}_4$  and 1.47mM of  $\text{KH}_2\text{PO}_4$ , with 0.905mM of  $\text{CaCl}_2$  and 0.492mM of  $\text{MgCl}_2$ ) and cultured in Normal Chicken Medium [M199 medium (Lonza #7331682) 10% Chicken Serum (Invitrogen #16110082) 5% Fetal Bovine Serum (Invitrogen #10500004) and 1% Penicillin/Streptomycin (Invitrogen #15140022)] on top of 0.8 $\mu\text{m}$  filters (Merck Millipore, #ATTP02500) floating on 200 $\mu\text{L}$  of medium, in 4-well plates (Thermo Scientific, #144444). Cultures had the duration of 6h or 12h, and were performed in an incubator (Nuair AutoFlow NU-4750 Water Jacket  $\text{CO}_2$ ) at 37°C, with a humidified atmosphere with 5%  $\text{CO}_2$ .

The explants were cultured under three different conditions. They were either cultured in Normal Chicken Medium, with 1% DMSO (Sigma, #D2650) or with 50 $\mu\text{M}$  of Rho Kinase Inhibitor III (RockOut, Merck Millipore #555553, dissolved in DMSO) added to this medium. Explant experiments were performed in two different ways, depending on what technique was used to analyze them: (1) explants to be processed for in situ hybridization were bisected along the axial structures (notochord and neural tube) and each half was cultured under one of two different conditions (control and experimental); (2) in order to preserve tissue architecture for immunolabelling and confocal analysis, explants were prepared and cultured as intact posterior portions of the embryo where control and experimental explants were from different individuals of the same stage. In both cases, two experimental groups were used, the first serving as a control for the potentially toxic effect of DMSO (Normal Chicken Medium vs DMSO) and the second as a test for the effect of RockOut (DMSO vs RockOut).

After culture the number of somites formed during culture was counted, using the nomenclature of Christ and Ordahl, 1995.

## In Situ Hybridization

### **Probe Production**

Probes for *Hairy1*<sup>17</sup>, *Hairy2*<sup>22</sup>, *Meso1*<sup>27</sup>, *Fgf8*, *Raldh2*, *Shh* and *Patched2* (referenced in Resende et al., 2010) were kind gifts from Isabel Palmeirim and Joaquín Rodríguez-León, and probes for *Itga5* and *Fn1* were generated in our lab<sup>55</sup>. An extended protocol for probe production can be found in supplementary protocols

### **Whole Mount *In Situ* Hybridization**

Embryos were collected and staged in DEPC-treated 1x PBS and fixed O/N in WISH [4% Formaldehyde (Sigma #F1635) in 150mM NaOH with 100mM EGTA (Sigma #E4378) in DEPC-treated water, to prevent mRNA deterioration]. Whole mount *in situ* hybridization was performed on HH10-14 embryos for all the probes mentioned previously. Whole mount *in situ* hybridization for *fn1* expression was also performed, in embryos staging from HH1 (first stage *in ovo*) to HH14.

After O/N fixation, embryos were dehydrated in methanol (50% first, then 2x 100% washes, 5 minutes each) and left at -20°C, at least O/N (and no more than 3 months).

On day 1 of the *in situ* hybridization protocol embryos were rehydrated in a 75%-50%-25% methanol series. After that they were bleached for an hour in 6% H<sub>2</sub>O<sub>2</sub> solution in Phosphate Buffer Saline (PBS) with 0.1% Tween (PBT). Embryos were then permeabilized with Proteinase K (Roche #3115879001) at 10µg/mL. Exposure times to Proteinase K depended on embryo stage (one minute per stage, i.e HH1=1 minute, HH10=10 minutes and so on). After that the embryos were post-fixed in 4% formaldehyde and 0.1% glutaraldehyde (Sigma #G5882) in PBT, to inactivate the Proteinase K and prevent deterioration of the tissues. Finally, embryos were passed through Hybmix by rinsing in a 1:1 PBT:Hybmix solution, and then left to incubate in Hybmix at 65°C/70°C for at least an hour. Instead of the incubation time, some embryos were put in Hybmix and stored at -20°C for future hybridization. After the 1h incubation they were submerged in 200-500µL of probe (depending on number of embryos per well/size of wells).

On day 2, the probe was recollected from the embryos and stored at -20°C to be reused. After that embryos were washed, for 30 minutes, twice in Post-Hybridization Mix (Post-Hybmix, 50% Formaline, 600mM NaCl, 60mM Trisodium Citrate and 0.2% Tween) at 65°C/70°C, and then transitioned to MABT (Maleic acid buffer solution, 100mM of Malic Acid, 150mM of NaCl, with 1% Tween) by washing in a 1:1 MABT:Post-Hybmix solution for 10 minutes at 65°C/70°C, and then twice in MABT. The embryos were then washed twice for one hour in blocking solutions, at room temperature (RT) and with agitation, first in a 2% Blocking reagent (Roche #11096176001) solution in MABT, and second in a 2% Blocking, 20% Sheep Serum (Sigma #S2263) solution in MABT. Finally, the embryos were incubated O/N, at 4°C, , with Anti-Digoxigenin-AP Fab

fragments (Roche #1093274) or Anti-Fluorescein-AP Fab fragments (Roche #11426338910), depending on the probe, diluted 1:2000 in 2% Blocking, 20% Sheep Serum solution in MABT.

On day 3, depending on how clean (less background) the probe's development is, embryos were either washed for ≈3h (often more) in MABT, or washed all day, several times, in MABT. In the last case, they were then stored O/N, at 4°C, in MABT, and the rest of the protocol happened on day 4. Embryos were then washed twice, for 10 minutes, at RT, in Alkaline Phosphatase (AP) Buffer (NTMT, 100mM MgCl<sub>2</sub>, 100mM Tris-HCl pH9,5, 100mM NaCl and 1% Tween, in H<sub>2</sub>O), and then developed in a 0.5mg/mL NBT (Roche #1383213) and 0.1875mg/mL BCIP (Roche #1383221) solution in NTMT.

To photograph, the AP reaction was either temporarily paused in MABT, or completely stopped in PBT. If paused in MABT, the reaction was continued incubating again in NTMT followed by NBT/BCIP solution in NTMT. After stopping the reaction in PBT and photographing the embryos, they were placed in 1% Sodium Azide in PBT at stored at 4°C.

## **Explant *In Situ* Hybridization**

After culture (6h or 12h) the explant's somites were counted in DEPC-treated 1x PBS, rinsed once or twice with DEPC-treated 1x PBS, and then fixed O/N in DEPC-treated WISH fixative.

Hybridization was performed with all the probes mentioned previously, in order to ascertain the influence of each culture condition on gene expression.

Explants were subjected to the exactly same protocol as intact embryos, except for Proteinase K incubation time, which was 10 minutes for all explants, regardless of their original stage.

Since not all explants ended up having a clear probe signal, and some explants were lost, broken or bent, only complete pairs of straight, well developed, explants were used to analyze the effects of each culture condition on gene expression.

## **Immunolabelling**

### **Whole Mount Immunolabelling**

Embryos ranging from HH1 to HH8 were processed for whole mount immunolabelling<sup>10</sup>, to analyze FN matrix deposition and fibrillogenesis. Embryos at stages HH10 and HH13 were also immunolabelled to compare somite morphology with that of cultured explants. Immunolabelling in these experiments was performed using, as primary antibodies, a rabbit anti-Fibronectin (Sigma #F3648 polyclonal antibody, at a 1:400 dilution and a mouse anti-N-Cadherin (BD Biosciences #610920) monoclonal antibody, at a 1:100 dilution in 1% ID (0,01g/mL Bovine Serum Albumin and 1% Tween in PBS). These dilutions were used to have a final concentration of about 15-25µg/mL of antibody. Secondary antibodies were an Alexa 488-coupled, goat anti-mouse antibody(Molecular Probes #A11017) and an Alexa 568-coupled, goat anti-rabbit antibody

(Alfagene #A21069) at a 1:1000 dilution in 1% ID in PBS. For nuclear staining we used the DNA-intercalator ToPro3 (Invitrogen #T3605).

Embryos were collected in complete PBS (with  $\text{Ca}^{++}$  and  $\text{Mg}^{++}$ ) and fixed O/N in 4% FISH (4% Paraformaldehyde, PFA, Merck #1030051000, with 4% Sucrose, 0.12mM of  $\text{CaCl}_2$ , 0.077mM of  $\text{Na}_2\text{HPO}_4$ , and 0.023mM of  $\text{NaH}_2\text{PO}_4$ ). On the next day they were washed briefly, several times, in Complete PBS, and then in 1% ID in PBS for 2 hours. After that the antibody solutions were prepared, and the embryos were incubated O/N, at 4°C (with or without agitation).

On the following day, embryos were washed extensively in Complete PBS, and then incubated in the secondary antibody solutions, which were made in 1% ID in PBS O/N, at 4°C (with or without agitation).

On the third day, embryos were washed several times in Complete PBS, then incubated O/N, at 4°C (with or without agitation) in a 1% ID solution containing 2 $\mu\text{M}$  of ToPro3 and 10 $\mu\text{g}/\text{mL}$  of RNase, to allow better intercalation of the ToPro with the DNA, and not with RNA.

On the final day, embryos were fixed in a 1% PFA solution (in the ID-diluted ToPro solution, to help maintain the staining in the nuclei) for 1-2h at RT, without agitation. After that, they were quickly washed in Complete PBS, and then slowly dehydrated in a 10% increment methanol series, or in a 10-20-40-60-80-100% methanol series. For the first series, transitions were made every 10 minutes, while for the second the first two transitions were 10 minutes apart, and the rest 20 minutes apart. Finally, they were laid to rest at -20°C until the day they were mounted in methyl salicylate and observed.

## **Explant Immunolabelling**

Whole posterior section explants were also immunolabelled in order to describe N-Cadherin, Fibronectin and Laminin protein distribution after culture. For this purpose, two combinations of primary antibodies were used: (1) anti-Fibronectin polyclonal antibody and the anti-N-Cadherin monoclonal antibody, previously mentioned; (2) mouse anti-Fibronectin (DSHB #B3/D6) monoclonal antibody and a rabbit anti-Laminin (Sigma #L9393) polyclonal antibody. Polyclonal antibodies were used at a 1:400 dilution, while monoclonal antibodies were used at a 1:100 (N-Cadherin) and 1:5 (Fibronectin) dilutions. These dilutions were used to have a final concentration of about 15-25 $\mu\text{g}/\text{mL}$  of antibody. Secondary antibodies were an Alexa 488-coupled, goat anti-mouse antibody and an Alexa 568-coupled, goat anti-rabbit antibody, and for nucleic staining we used the DNA-intercalator ToPro3.

Collected explants were washed in Complete PBS to remove the leftover medium and their somites were counted. Afterwards they were fixed O/N in 4% FISH. The rest of the protocol was performed as previously described for whole mount immunolabelling.

## **Image Acquisition and Treatment**

### **Stereoscope Microscopy**

Stereoscopic imaging was performed in a Zeiss Lumar.V12 with a ImagingSource DFK 23U274 camera, coupled to a 0,63x coupling ring, through a ApoLumar S 1,2x FWD 47mm lens.

Image acquisition was done through the IC Capture V2.3 software and image processing was done using the FIJI software. To allow better comparison of the expression patterns, PSM's were straightened with the FIJI plugin "Straighten" and aligned by s0, marked by a white dashed line in the images.

### **Confocal Microscopy**

Confocal imaging was performed using a Leica DMI 4000B microscope coupled with a Leica TCS SPE scanner head, either using a 20x, 0.7 NA air APO CS lens or a 40x, 1.15 NA oil ACS APO lens. Images were acquired with the LAS AF software and processed using the Amira v5.3.3 software. Reconstructions of matrix protein labelling and merged images represent the ventral one-third to half of the somite, while N-Cadherin labelling reconstructions represent the medial three-quarters of the somite.

# Results

## Expression pattern of *fn1* and *itga5*, key genes involved in FN matrix assembly

As previously mentioned, the FN matrix plays a very important role during somitogenesis. It has been extensively shown that a FN matrix is primarily assembled through integrin  $\alpha5\beta1$ -mediated ligation and extension of the FN dimer<sup>63,70-74</sup>. To better understand the role of this matrix during somitogenesis, we decided to analyze how it is set up from the earliest stages of development of the chick embryo until the formation of 13-15 somites. We started with the earliest available stage to us, HH1, and followed the expression of *fn1* and *itga5* until stage HH12. At stages HH1 to HH3, *fn1* is expressed in a punctuated, “salt-and-pepper” pattern (Fig. 4 A-C), while *itga5* expression seems to follow the establishment of the primitive streak (Fig. 4 G-I).

As the primitive streak expands rostrally the punctuated expression of *fn1* also moves rostrally, while more caudally the expression becomes restricted to the primitive streak and becomes uniform (Fig. 4 D, arrowheads). *fn1* also starts to be expressed around the embryo, in the anterior two-thirds of the extraembryonic tissues. *itga5* continues to only be expressed in and around the primitive streak, although its expression is almost nonexistent in the most caudal part of the primitive streak (Fig. 4 J, arrowhead). At stage HH5 gastrulation has already started in the most rostral region of the embryo, and cephalic mesoderm and the primordial cephalic neuro epithelium have formed rostrally. At this stage *fn1* expression in the extraembryonic tissue has almost reached the most caudal point of the embryo, while the punctuated expression pattern in the more rostral region has practically disappeared (Fig. 4 E). Both *fn1* and *itga5* are still being expressed in the primitive streak, although now they show an expression gradient that increases from posterior to anterior, being strongest in the most rostral region of the streak, closest to the node (Fig. 4 E, K, arrowheads). As gastrulation proceeds and the node regresses along the primitive streak, *fn1* expression becomes increasingly caudal. At stage HH6 *fn1* expression has reached the most caudal region of the extraembryonic tissues, and starts being expressed in the remaining caudal epiblast, forming a V-shaped expression pattern (Fig. 4 F). Expression also becomes more intense in the border between the neuroepithelium and the epidermal ectoderm, where a very dark band of expression is found (Fig. 4 F, arrowhead). At these stages, *itga5* starts to be expressed in the cephalic neuroepithelium (Fig. 4 L, arrowhead).

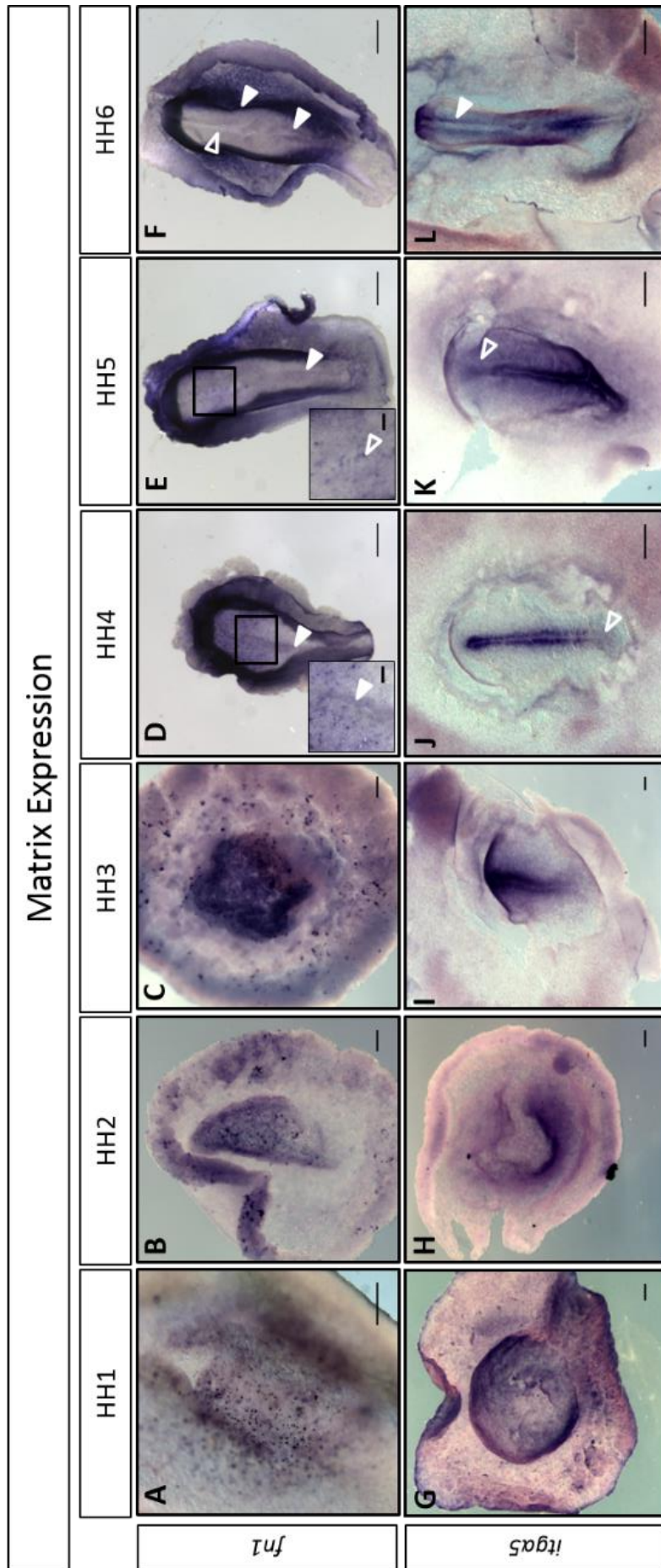


Figure 4 - Expression patterns of the matrix gene *fn1* and its integrin receptor, *itga5* from HH1 to HH6. (A-F) *fn1* expression pattern. (G-L) *itga5* expression pattern. (A-C) *fn1* starts to be expressed in a sparse salt and pepper pattern and slowly becomes denser and expands to all the embryonic tissue. (D-E) *fn1* punctuated expression becomes less and less evident in the anterior of the embryo, while being maintained around the primitive streak. (G-I) *itga5* expression seems to follow the primitive streak formation, being expressed in its crests. (K, L) *itga5* expression disappears from the midline of the embryo in areas where gastrulation has occurred, but later reappears in the neuroepithelium. Full arrowheads represent areas of expression of the respective gene, while hollow arrowheads represent areas without or with weak expression. Scale bar represents 200  $\mu$ m for A-C, G-I; 500  $\mu$ m for D-F, J-L; and 100  $\mu$ m for the amplifications in D and E.

Starting at stage HH7 we can clearly see that the epidermal ectoderm strongly expresses *fn1*, but the neuroepithelium shows no sign of expression, and the intense expression in the border between these two tissues becomes clearer (Fig. 5 A-E, arrowheads). At this same stage, *itga5* has started being expressed in the most caudal PSM, as well as in somites, lateral mesoderm and around the node, and this expression is maintained at least until stage HH12 (Fig. 5 G-L). During stage HH8 and HH9 *fn1* expression starts to decrease in the epiblast as this tissue disappears, and epidermal ectoderm expression becomes more medial as the neural tube starts to close (Fig. 5 B, C). Somites also start to show expression of *fn1* at this stage (Fig. 5 C, arrowhead). From stage HH10 to HH12 this expression pattern is maintained, while *fn1* expression becomes increasingly strong in the heart primordia (Fig. 5 D-F, arrowheads).

## Matrix Assembly

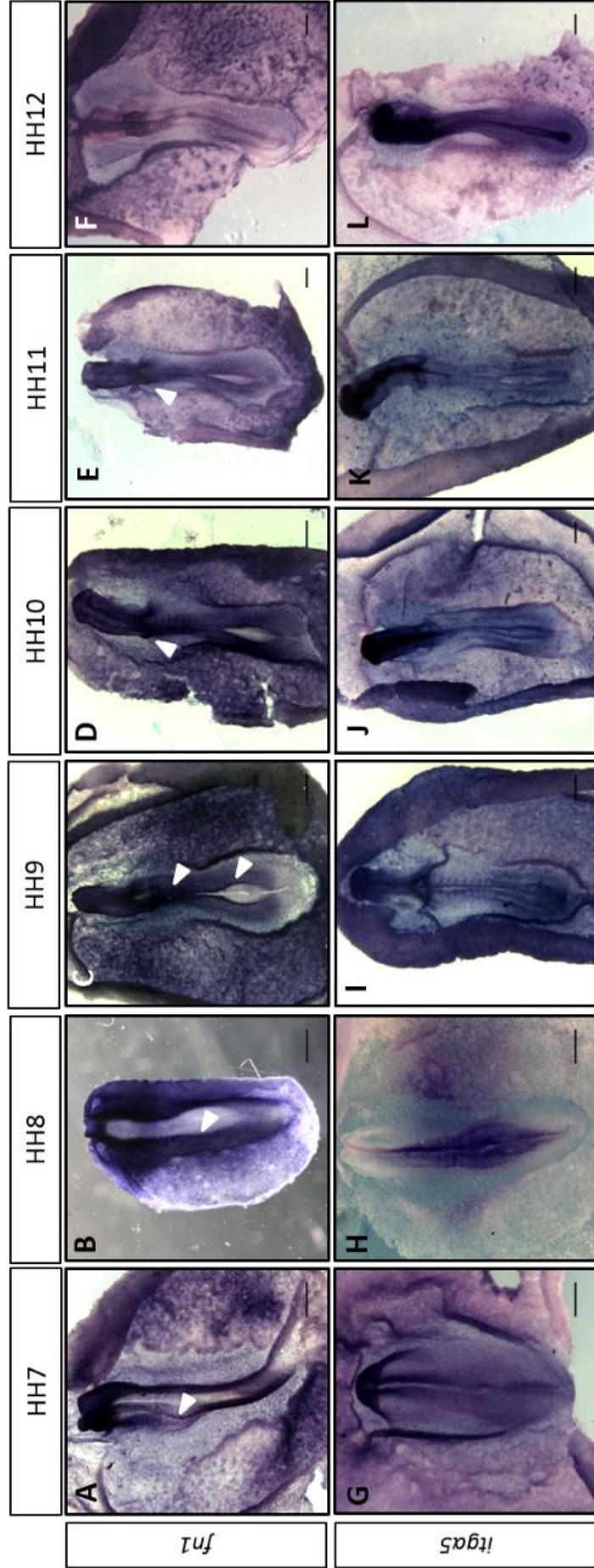


Figure 5 - Expression patterns of the matrix gene *fn1* and the gene *itga5*, codifying the  $\alpha$  subunit of its integrin receptor, from HH7 to HH12. (A-F) *fn1* expression pattern. (G-L) *itga5* expression pattern. (A-C) A band of strong expression of *fn1* becomes increasingly evident in the frontier between epidermal ectoderm and neuroepithelium. (G,H) *itga5* becomes more expressed in the paraxial mesoderm. (D-F) *fn1* expression starts to become apparent in the forming heart primordia. Full arrowheads represent areas of expression of the respective gene, while hollow arrowheads represent areas without, or with weak expression. Scale bar represents 500  $\mu$ m in all images.

## FN matrix assembly and development

To determine how the matrix assembly correlates with the expression pattern of both genes we performed whole mount immunofluorescence in two representative stages, stage HH4, when the embryo is preparing to start gastrulation, and stage HH8, when gastrulation is still proceeding caudally and somitogenesis and heart formation are underway. At stage HH4 we can see that there is more labelling of FN in the rostral part of the embryo than in the caudal region, and we can also distinctly see a gradient of matrix assembly around the primitive streak, but nowhere else (Fig. 6 B, arrowheads). This pattern is overlappable with the expression patterns of both *fn1* and *itga5* described above for this stage (shown in Fig. 5 A,C), suggesting that these genes expression patterns are intimately correlated with FN matrix deposition and assembly at this stage.

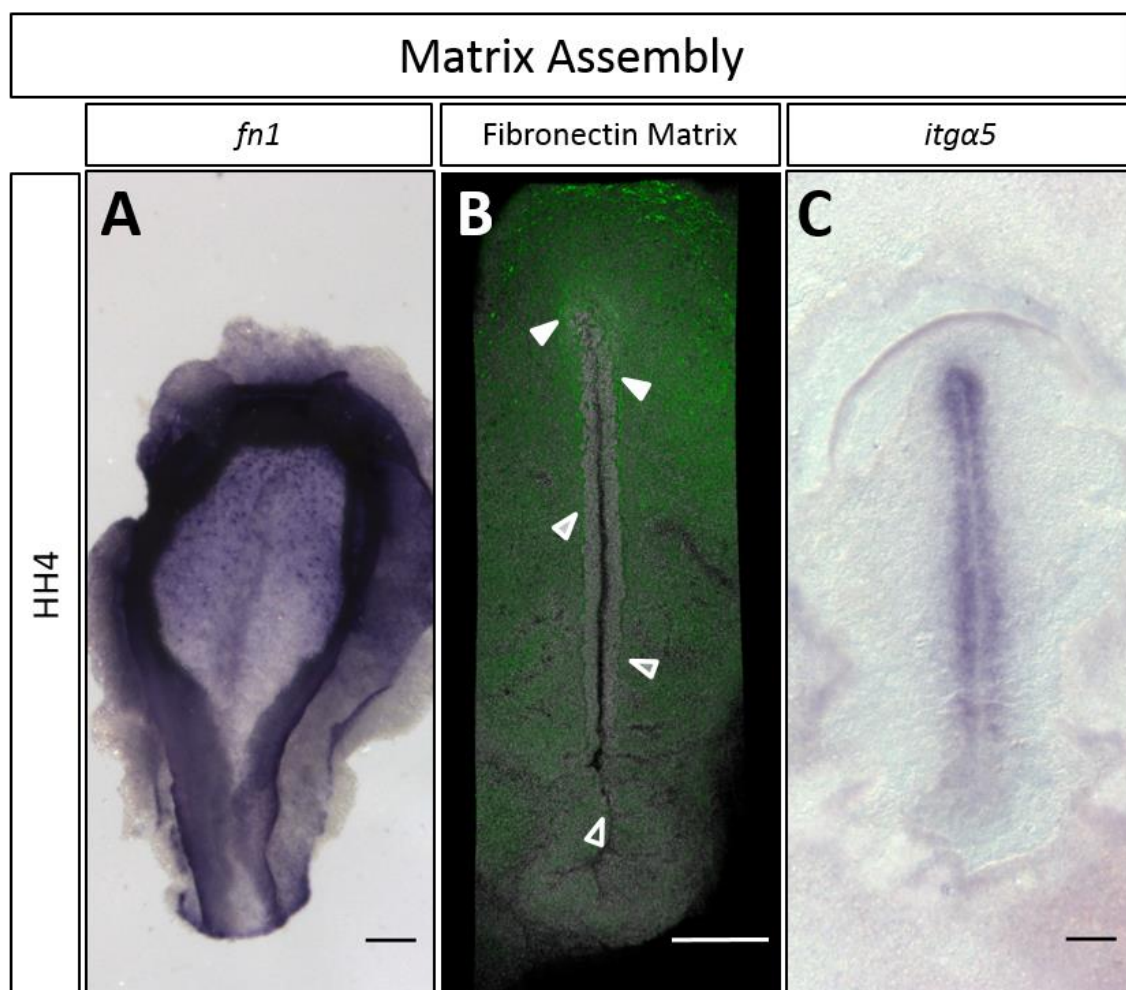


Figure 6- Comparison of *fn1* and *itga5* gene expression with assembly of FN matrix at stage HH4. (A) *fn1* expression pattern. (B) FN matrix deposition and assembly pattern. (C) *itga5* expression pattern. Matrix deposition and assembly seems to follow both *fn1* and *itga5* expression patterns, suggesting a relation between the expression of both genes and the assembly of the FN matrix. Full arrowheads represent areas of dense protein deposition, while progressively more hollow arrowheads represent areas of progressively sparser protein. In B, green represents FN marking and grey represents nuclear staining. Scale bar represents 250 $\mu$ m in all images.

To check if the expression patterns were actually indicative of the matrix assembly pattern across early development we decided to perform the same experiment on a later stage, where more organogenic processes are under way. For the reasons mentioned above, we chose stage HH8. At stage HH8 a high degree of FN matrix assembly is observed in the rostral half of the embryo, particularly in the head, primordial heart and around formed somites. As we move caudally, labelling becomes less intense and the matrix seems less assembled, congruent with our observations made at stage HH4 and the expression patterns of both genes at stage HH8 (Fig. 7 B, arrowheads). Again, this FN matrix deposition and assembly patterns seem to be, mostly, correlated with the expression patterns of the genes in study. However, at this stage we can clearly start to see that there is FN matrix being assembled in places where there is no *fn1* expression, but where *itga5* is expressed. These results indicate that FN protein can be exchanged between tissues in the early embryo.

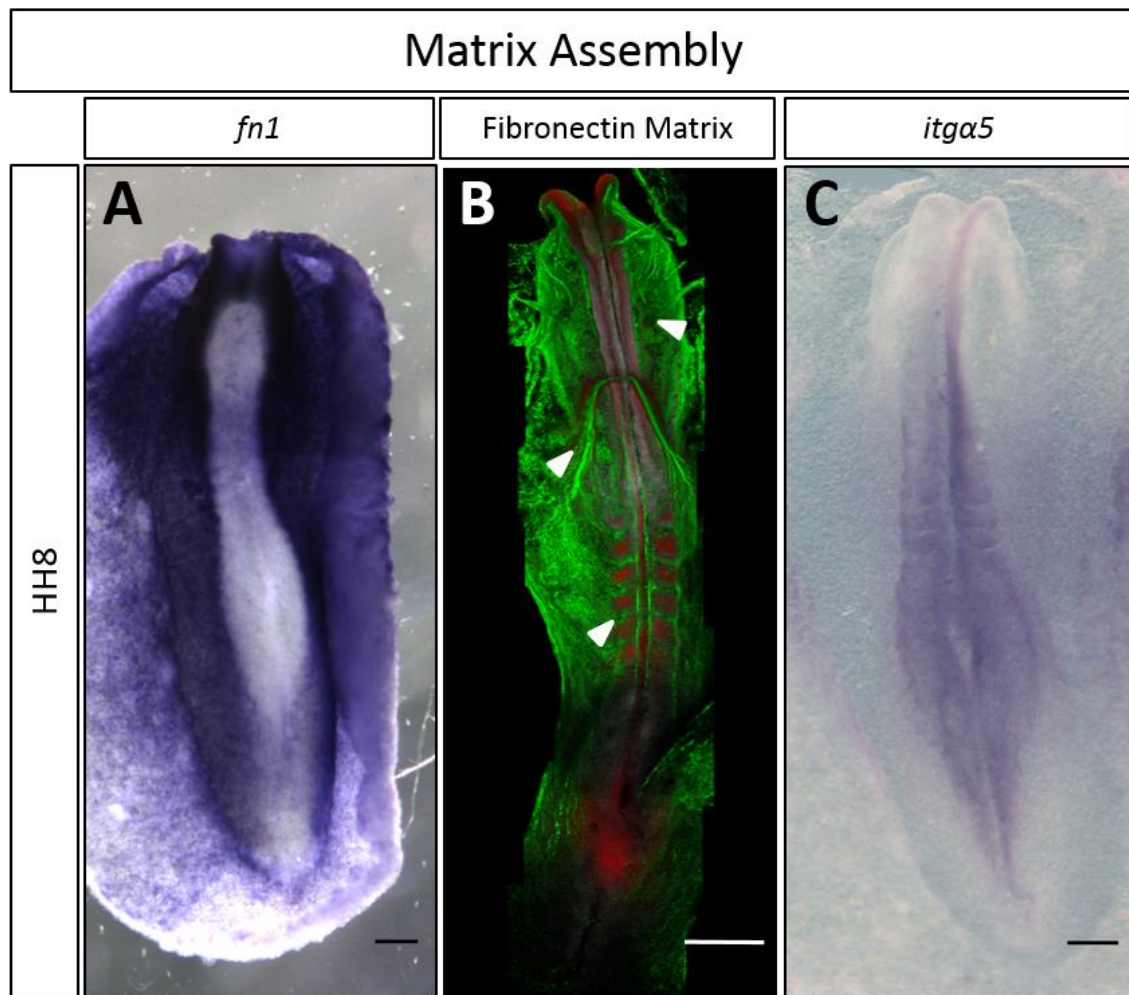


Figure 7 – Comparison of *fn1* and *itga5* gene expression with assembly of FN matrix at stage HH8 (A) *fn1* expression pattern. (B) FN matrix deposition and assembly pattern. (C) *itga5* expression pattern. Again, both expression patterns correlate with matrix assembly. However, now we can see that there is assembly of FN matrix in places where there is no *itga5* expression, indicating the participation of other known receptors. In B green represents FN labelling, red represents N-Cadherin labelling and grey represents nuclear staining. Full arrowheads represent areas of dense protein deposition. Scale bar represents 250 $\mu$ m in all images.

## Culturing with RockOut, a cellular tension-reducing drug

### Effects of loss of tension in somite formation, maturation, and matrix assembly

With the previous observations we give further evidence that during early chick embryo development *fn1* expression and FN matrix assembly exists in a gradient that decreases from rostral to caudal. As detailed before, it has been suggested that a gradient of tension exists in the embryo at these stages, suggesting that processes such as e.g. somitogenesis might be, in some way, regulated or influenced by this gradient. To test whether cellular tension indeed plays a role at these stages, and focusing on somitogenesis, we examined the effect of RockOut, a ROCK kinase inhibitor, which prevents non-muscle myosin II phosphorylation and assembly, on two processes: (1) the morphology of somite formation, and (2) gene expression of PSM and somites. By inhibiting non-muscle myosin-II phosphorylation and assembly we are interfering with the ability of the cell to contract and, therefore, exert tension upon the matrix.

We decided to examine the effect of the inhibitor on the ability of the somite to form a sphere of polarized epitheloid cells<sup>10</sup>. In addition, we also assessed the effects of the RockOut treatment on matrix assembly. For that purpose we chose to examine the FN matrix, and also the LN matrix, another major, and very important, component of the extracellular matrix around the somites<sup>64</sup>.

We cultured explants of caudal parts of embryos, as previously described, and performed immunofluorescence labeling against FN and N-Cadherin, or FN and LN, and selected somites at certain levels to compare, always from the left side of the embryo (to standardize). We selected somite sII and s-II and also s-IV (when existent, i.e. 12h cultures) pre-culture. These specific somites were chosen because sII represents a somite formed before culture, s-II represents a somite formed during culture but whose PSM region was already determined at the moment culture started, and s-IV represents a somite that was both formed, and derived from PSM determined, after the culture was initiated, allowing us to test the effect of RockOut treatment over three distinct stages of somite formation.

After 6h culture, sII (which became sV or sVI after culture, Fig. 8) control and DMSO somites show a dense FN matrix, especially on their lateral side, while the medial side shows a slightly less assembled matrix, with several aggregates of globular FN (Fig. 9 and 10 A, B, M, N). Epithelialization seems to be rather variable, with somites showing better or worse definition of the somitocoel, but in any case most show a higher degree of N-Cadherin deposition in the dorso-medial region of the somite (Fig. 9 G, H) than in other regions. The LN matrix, in turn, shows less assembly and compaction than FN, as previously described (Fig. 10 G, H, M, N, and Rifes and Thorsteinsdóttir, 2012). s-II (after, sI or sII, Fig. 8) shows, overall, the same conditions as sII, but with a slightly less compact FN matrix (Fig. 9, 10 D, E, P, Q), a slightly less organized epithelialization (Fig. 9 J, K), and also a less compact LN matrix (Fig. 10 J, K, P, Q).

As for RockOut treated-explants, both sII and s-II, after 6h culture, show less assembly of the FN matrix, with more globular aggregates, particularly noticeable in the lateral side and the ventro-medial side of the somites (Fig. 9, 10 C, F, O, R). Both also show a generalized N-Cadherin staining, all around the edge of the somite, which is a compact agglomerate of cells, with no

discernable somitocoel (Fig. 9 I, L). Interestingly, the LN matrix is much denser in explants cultured with RockOut compared to control explants, especially in the most medial region (Fig. 10 I, L, O, R).

After 12h culture, sII (after, sVII to sX, Fig. 8), s-II (after, sIII to sVI, Fig. 8) and s-IV (after, sI to sIV, Fig. 8) of control and DMSO explants all show the same progression of protein assembly and deposition observed at 6h, with the oldest somites showing a more dense FN matrix than the youngest, as well as a better defined epithelialization (Fig. 11, 12, except C, F, I, L, O, R, U, X, P). However, this is best observed on the dorsal side of the somites (data not shown), and only slightly at the ventral side, because the FN matrix is starting to disassemble medially, and in older somites also more ventrally, in preparation for sclerotome differentiation and expansion<sup>5</sup>. It should be noted that at 12h there is more variability in terms of effects of the treatment than observed at 6h, with some explants having almost no matrix around the paraxial mesoderm, while others have almost normal amounts of protein. However, upon closer inspection, it is evident that the matrix shows a much lower degree of assembly, and has a very different structure than the one observed for control somites. Furthermore, RockOut cultured somites seem to have less matrix around their ventral sides at all time points, suggesting that lack of tension also interferes with the transportation of the protein to that side of the somite.

This lack of matrix leads to some defects. First, as is the case with the somite shown in Figure 11 F, O and X, several RockOut treated explants show fused somites (21% of somites, n = 43; compared to 3.3% of somites in control explants, n = 240; normal medium and medium with DMSO), indicating a failure in the maintenance of somitic clefts (Fig. 11 C, F, I, U, X, P). Although not all somites show such a strong a consequence of impaired matrix assembly, they still have a higher globular/fibrillar ratio than their control counterparts, and seem delayed in assembling the typical matrix organization necessary for sclerotome development (Fig. 12 C, F, I, U, X, P). Second, although somites treated with RockOut have recovered somewhat from the epithelialization defect observed at 6h they still seem to have a slightly less defined epithelialization than their control counterparts (Fig. 11 L, O, R). Finally, the LN matrix is not as dense as at 6h of culture, although it still looks slightly denser than in the control and DMSO somites (Fig. 12 L, O, R, U, X, P).

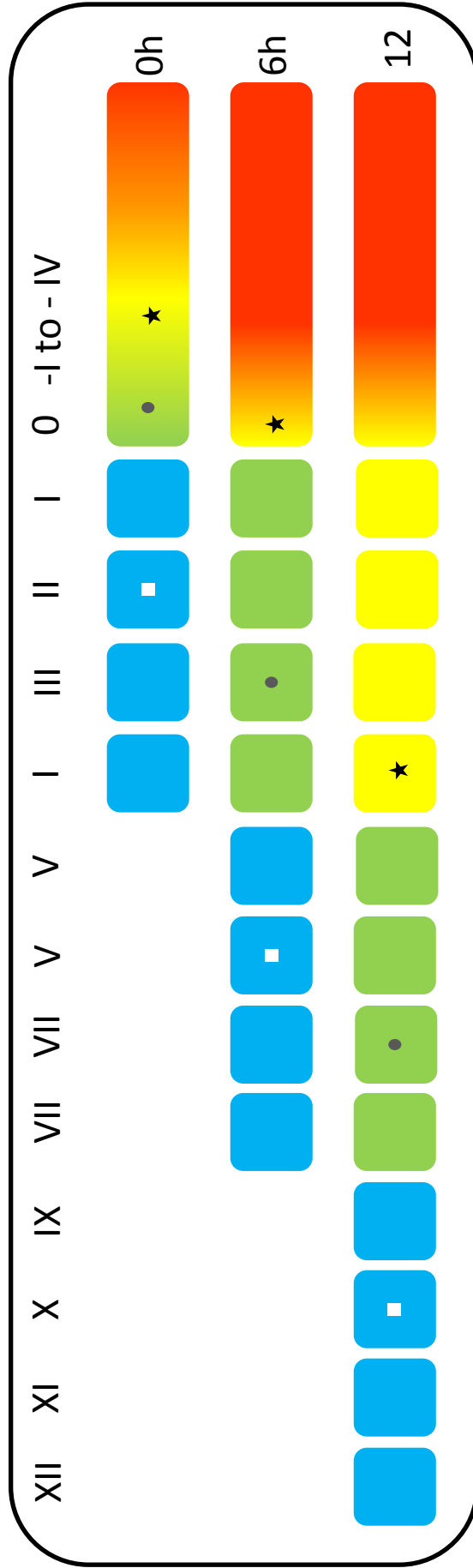


Figure 8 - Schematic representation of relative development of each axial level of the presomitic mesoderm after each culture period. Red represents cells that never become determined mesoderm. Yellow represents cells that become determined mesoderm during the culture period. Green represents cells from mesoderm determined prior to culture. Blue represents cells that had already formed a somite prior to culture. Roman numerals are used to name each somite according to its formation time. The white square, ball and star were used to represent cells from the same starting axial level at different timepoints in the development, after culture.

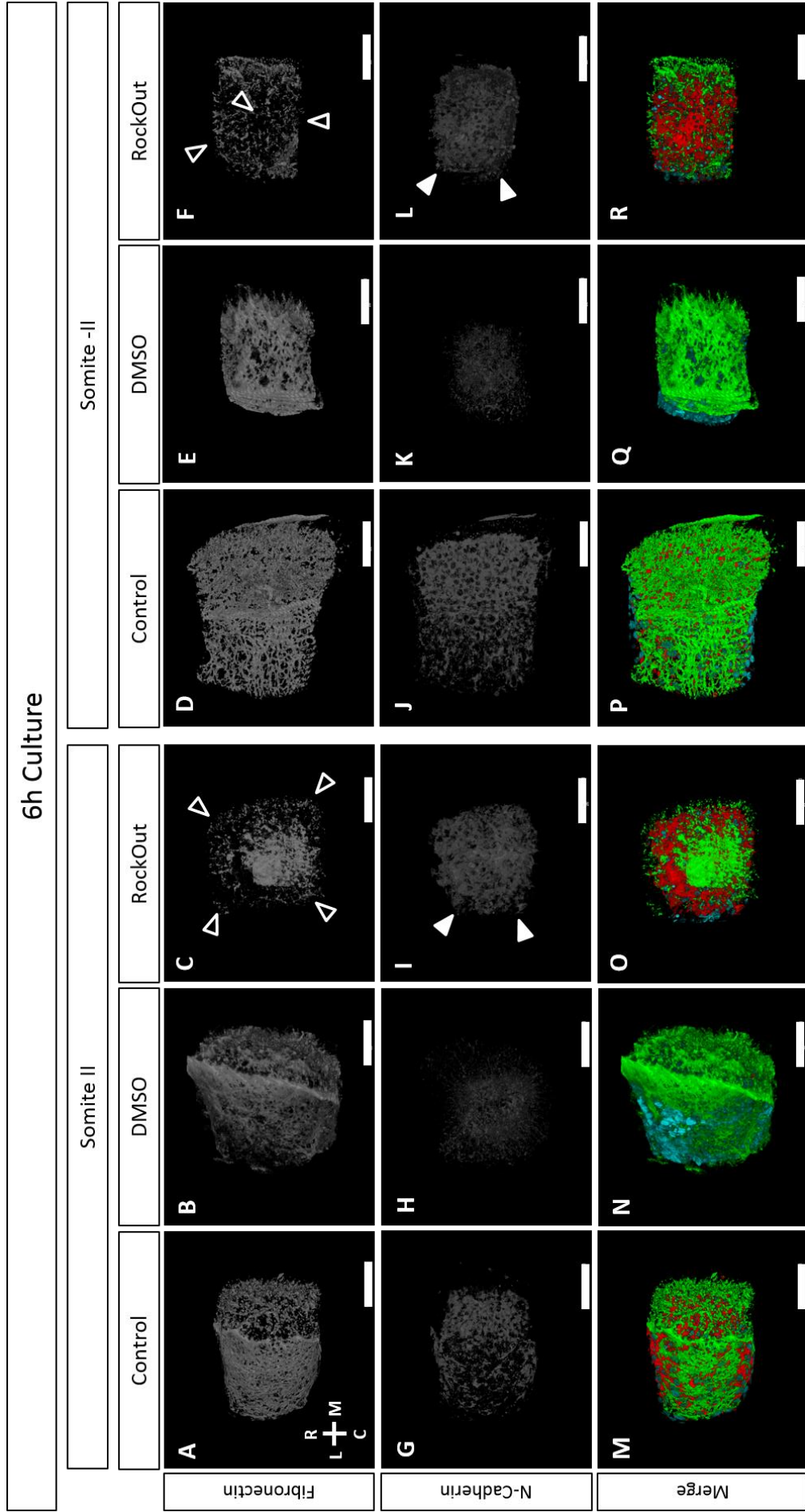


Figure 9 – At 6h of RO culture there is a clear reduction in FN matrix assembly, as well as a perturbation of the epithelialization of the somite. Nuclear staining is in blue, N-Cadherin deposition in red and FN matrix in green. Full arrowheads indicate areas of dense deposition of protein, hollow arrowheads indicate areas of sparse protein deposition. R – Rostral, C – Caudal, L – Lateral and M – Medial. All scale bars represent 20µm.

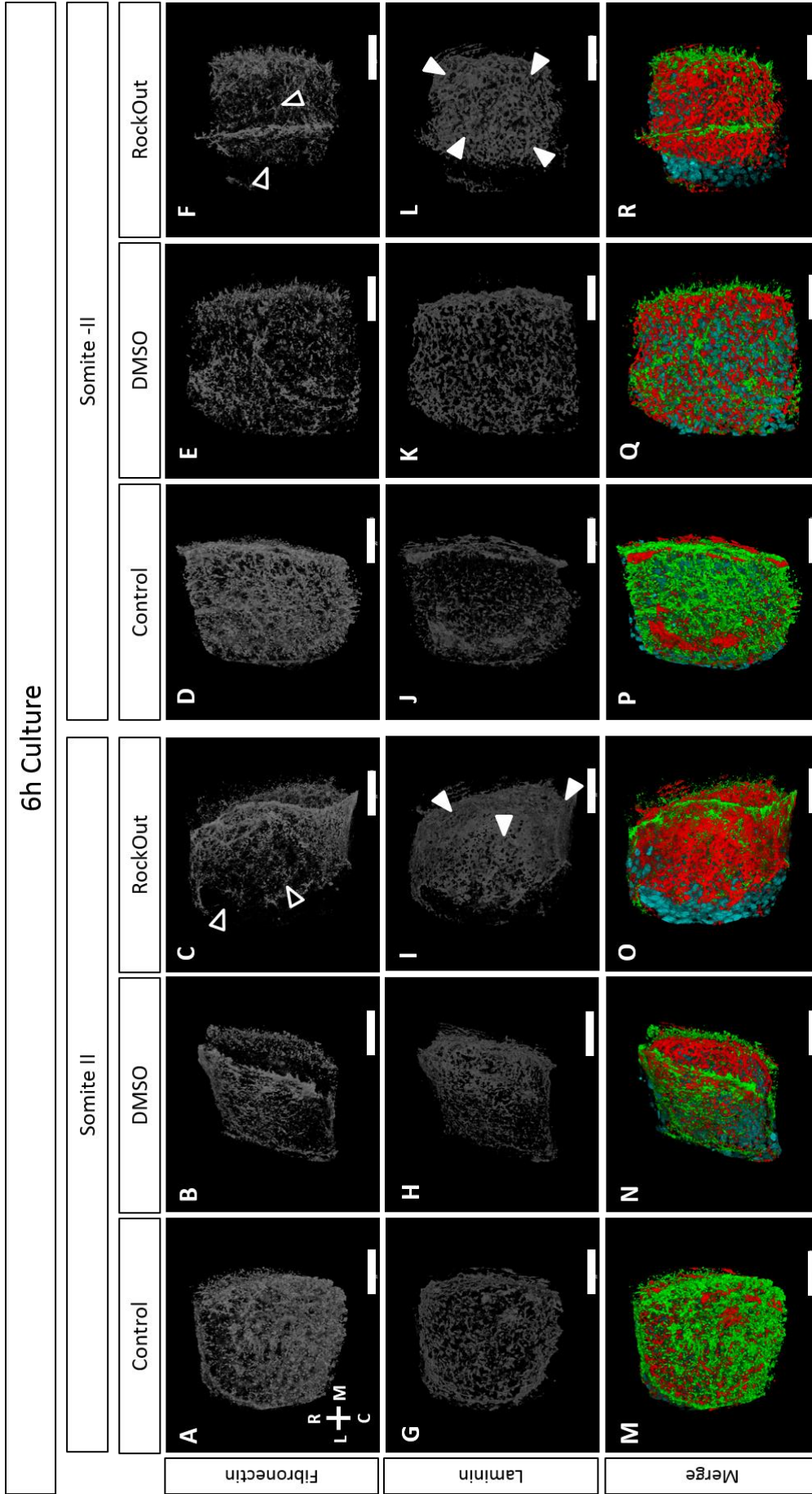


Figure 10 – After 6h culture, while the FN matrix shows less assembly, the LN matrix seems to become denser, in particular in the medial region. Nuclear staining is in blue, LN matrix deposition in red and FN matrix in green. Full arrowheads indicate areas of dense deposition of protein, hollow arrowheads indicate areas of sparse protein deposition. R – Rostral, C – Caudal, L – Lateral and M – Medial. All scale bars represent 20µm.

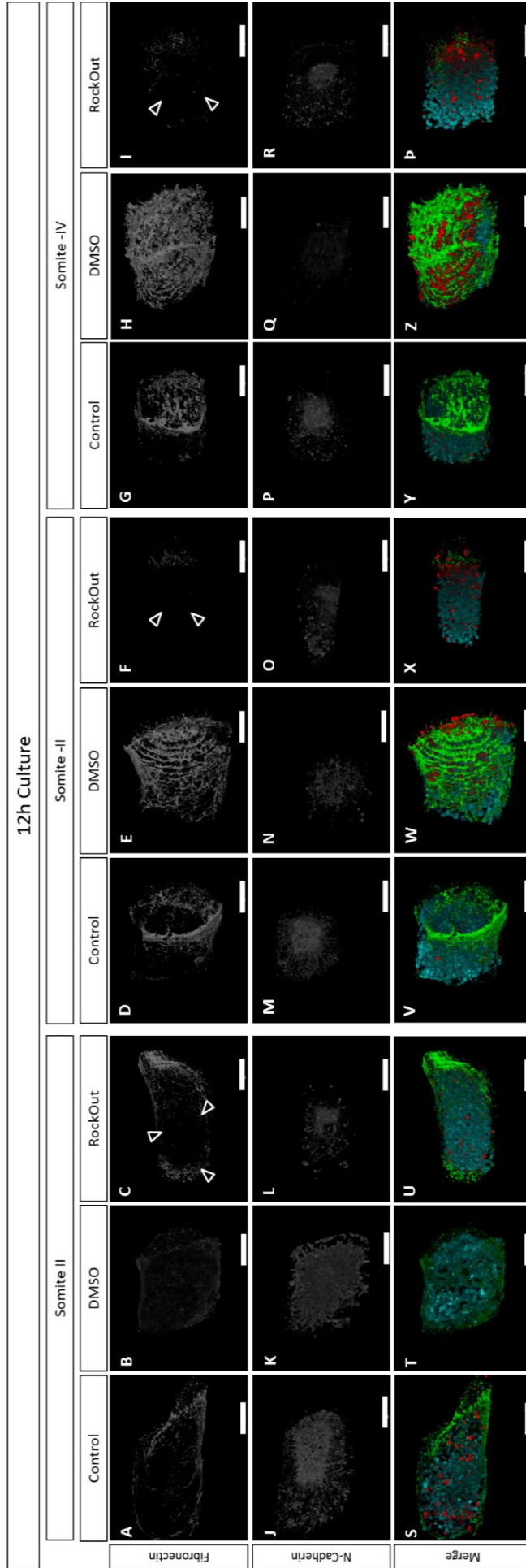


Figure 11 – 12h RO cultured explants also show less assembly of the FN matrix, which at this time also becomes sparser in general, in the ventral side. Epithelialization seems to recuperate partially, but still looks less extensive than in the controls. Nuclear staining is in blue, N-Cadherin deposition in red and FN matrix in green. Full arrowheads indicate areas of denser deposition of protein, hollow arrowheads indicate areas of sparser protein deposition. R – Rostral, C – Caudal, L – Lateral and M – Medial. All scale bars represent 20µm.

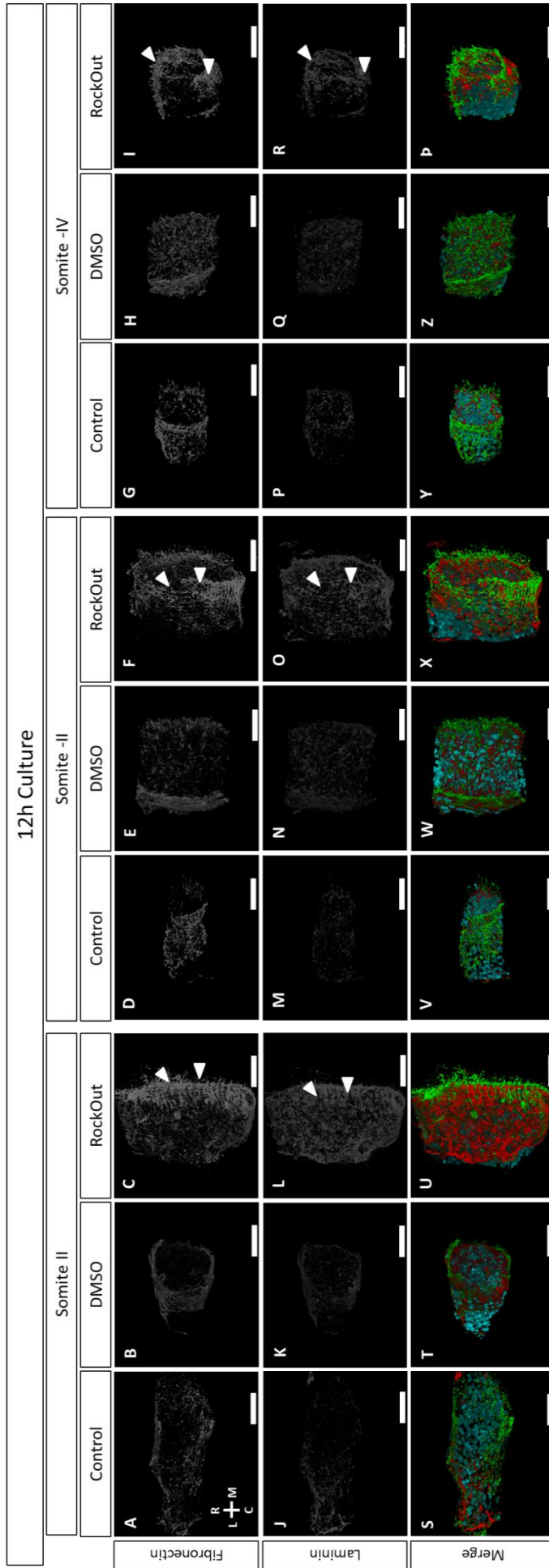


Figure 12 – FN matrix shows a great level of disassembly when cultured for 12h with RO, as well as an altered deposition pattern, while LN seems to become more similar to the control, when compared to the results after 6h of culture. (Nuclear staining is in blue, LN matrix deposition in red and FN matrix in green. Full arrowheads indicate areas of dense deposition of protein, hollow arrowheads indicate areas of sparse protein deposition. R – Rostral, C – Caudal, L – Lateral and M – Medial. All scale bars represent 20µm.

## Effects of loss of tension on gene expression during somitogenesis

Since explant cultures with RockOut affected both the epithelialization of somites and matrix assembly, we decided to test whether or not the lack of cellular tension would also have an effect on the expression of genes already known to regulate somitogenesis. To assert this we performed *in situ* hybridizations against *shh*, *ptchd2*, *fn1*, *itga5*, *fgf8*, *raldh2*, *hairy2* and *meso1* in bisected explants, cultured for 6h or 12h. Because bisecting the explants means dividing the axial structures in half, and Shh signaling plays a role in somite development, we decided to first check the expression of *shh*, to make sure that the notochord was being properly divided, and *ptchd2*, to determine if tissues on both sides were receiving notochordal Shh. As can be seen in Fig. 13 and 14, which show representative results obtained for hybridized explants (*shh* n= 10; *ptch2* n= 11), both the notochord and Shh signaling seem to be mostly intact, and equally distributed between both explants, indicating that they are correctly divided.

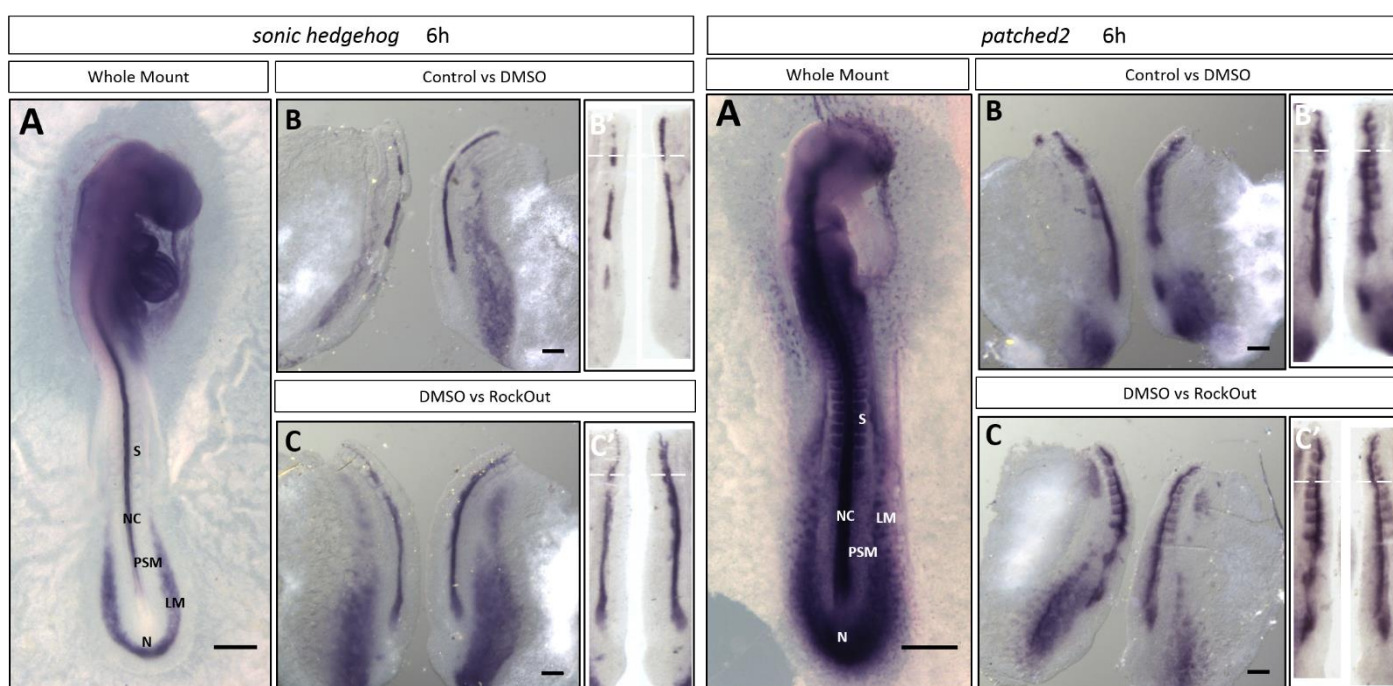


Figure 13 - *shh* expression pattern in explants cultured for 6h, showing expression of *shh* in both halves of the bisected explants. (A) *shh* expression in an intact nonmanipulated embryo for comparison. (B,B') *shh* expression in a control pair of explants, to rule out DMSO effects. (C,C') *shh* expression pattern in an experimental pair of explants, to assess RockOut effects. (B',C') Straightened paraxial mesoderms from B and C, respectively, to allow comparison of axial extension and position of the pattern. S – Somite, NC- Notochord, PSM – Pre-Segmented Mesoderm, LM – Lateral Mesoderm, N – Node. Scale bar represents 500 $\mu$ m in A and 200 $\mu$ m in B and C.

Figure 14 - *ptchd2* expression pattern in explants cultured for 6h, showing expression of *ptchd2* in both halves of the bisected explants.. (A) *ptchd2* expression in an intact nonmanipulated embryo for comparison. (B,B') *ptchd2* expression in a control pair of explants, to rule out DMSO effects. (C,C') *ptchd2* expression pattern in an experimental pair of explants, to assess RO effects. (B',C') Straightened paraxial mesoderms from B and C, respectively, to allow comparison of axial extension and position of the pattern. S – Somite, NC- Notochord, PSM – Pre-Segmented Mesoderm, LM – Lateral Mesoderm, N – Node. Scale bar represents 500 $\mu$ m in A and 200 $\mu$ m in B and C.

Our first observations, when performing explant cultures, were that RockOut-treated explants form, on average, a lower number of somites during culture for both 6h and 12h (Fig. 15 and 16). We then performed *in situ* hybridizations to detect *fn1* and *itga5* expression, which showed similar expression patterns between control and RockOut treated explants, both after 6h and 12h (Fig. 17 and 18), indicating that the expression of these genes is not being significantly influenced by the lack of tension, at least not within this time frame.

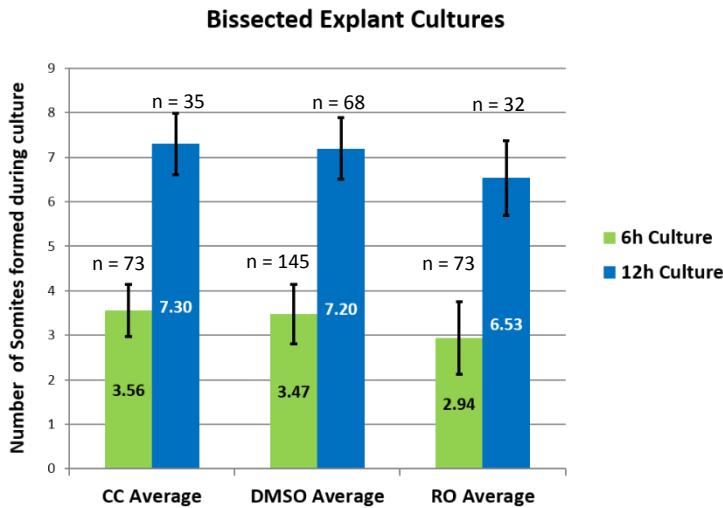


Figure 15 - Average number of somites formed during culture for each culture condition and time period, showing a decrease of the number of somites formed in explants cultured with RO. Numbers in the center of the bars represent the average number for that culture period and treatment, the black bars represent standard deviation from the average and each sample size is discriminated above each corresponding bar (n=).

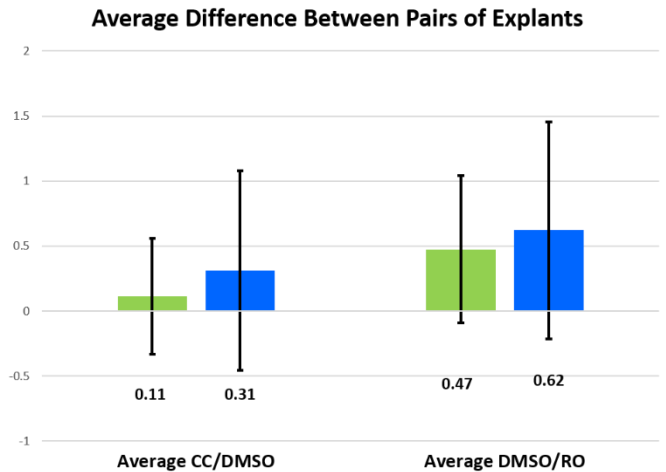


Figure 16 - Average difference of somites formed between each experimental pair of explants, demonstrating that experimental pairs have a higher difference in the number of somites formed than the control pairs. After culture the number of somites formed by each individual half of the explant was counted. The number of somites formed by the experimental half (DMSO or RockOut) was then subtracted to the number of somites formed by its corresponding control half (CC or DMSO), and the average of these differences was calculated for each experimental group and for each time period. Black bars represent standard deviation. Negative values are real and represent situations where the experimental half formed more somites than its control.

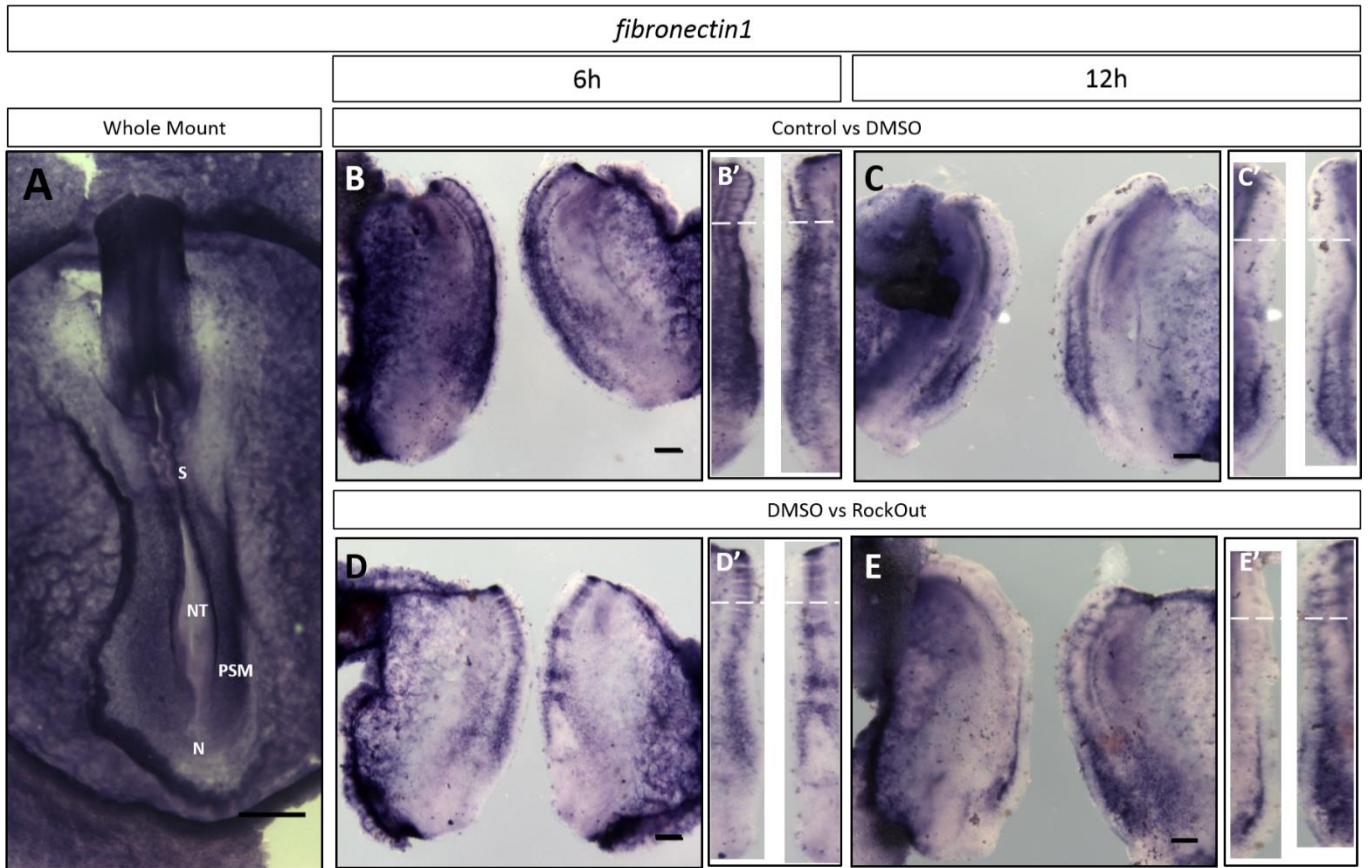


Figure 17 - *fn1* expression pattern in explants cultured for 6h or 12h. Apparently lack of tension does not lead to alterations on the expression pattern and intensity of *fn1*. (A) *fn1* expression in an intact nonmanipulated embryo for comparison. (B,B',C,C') *fn1* expression in control pairs of explants, to rule out DMSO effects. (D,D',E,E') *fn1* expression pattern in experimental pairs of explants, to assess RockOut effects. (B',C',D',E') Straightened paraxial mesoderms from B, C, D and E, respectively, to allow comparison of axial extension and position of the pattern. S – Somite, NT- Neural Tube, PSM – Presomitic Mesoderm, N – Node. Scale bar represents 500µm in A and 200µm in B,C, D and E.

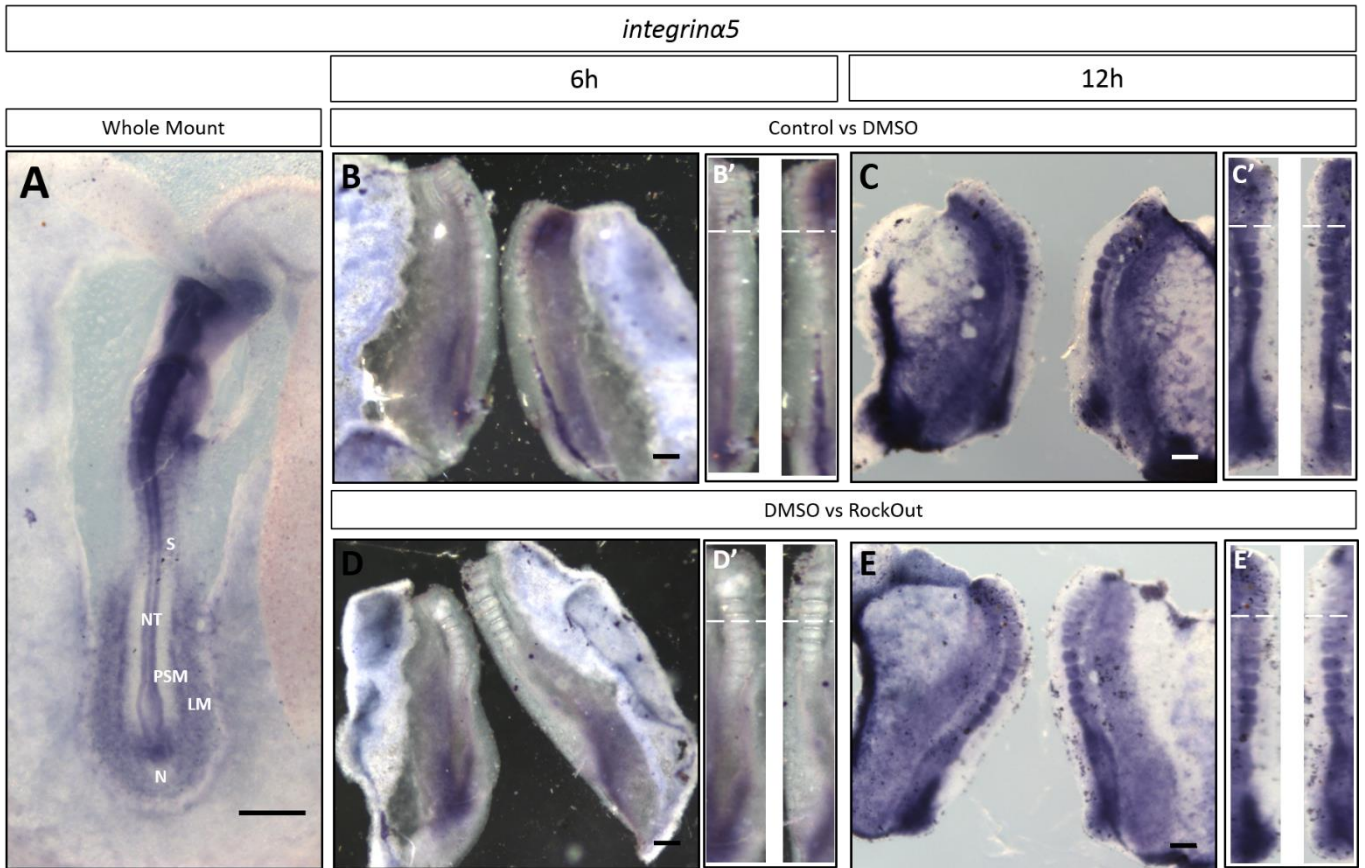


Figure 18 - *itga5* expression pattern in explants cultured for 6h or 12h. Lack of tension seems to not lead to an increase of expression of FN receptor in the PSM. (A) *itga5* expression in an intact nonmanipulated embryo for comparison. (B, B', C, C') *itga5* expression in control pairs of explants, to rule out DMSO effects. (D, D', E, E') *itga5* expression pattern in experimental pairs of explants, to assess RockOut effects. (B', C', D', E') Straightened paraxial mesoderms from B, C, D and E, respectively, to allow comparison of axial extension and position of the pattern. S – Somite, NT- Neural Tube, PSM – Presomitic Mesoderm, LM- Lateral Mesoderm, N – Node. Scale bar represents 500µm in A and 200µm in B, C, D and E.

We then tested the expression of a group of genes that regulate somitogenesis. We started by testing the influence of lack of tension in the determination of PSM cells. To that end, we performed hybridizations against *fgf8*, a marker for undetermined paraxial mesoderm, and *raldh2*, expressed in epithelialized somites. Both genes seem to show a slight rostral advancement of their expression patterns in RockOut-treated explants compared to the controls (Fig. 19 and 20, arrows). This is visible in Fig. 19 D' and E', where we can see that the staining reaches more anteriorly in the experimental half (right) than in the control (left; arrows), and also in Fig. 20 C', where the experimental side shows a less caudal expansion of expression than the control (arrows), suggesting that cells may remain undetermined for longer in the PSM when tension is blocked (n= 4 in 6 explant pairs for *fgf8*, and n= 2 in 3 pairs for *raldh2*).

Lastly we decided to test if there was any effect on the expression of the cycling genes, *hairy2* and *meso1*. Like the name indicates, both genes show a cycling pattern of expression, which means that a change in tempo is not only visible in a change on the R-C axial expression pattern, but also by both explants having different patterns of expression (different phases of the clock, Palmeirim et al., 1997). The expression pattern of *hairy2* and *meso-1* are indeed different between the controls and the RockOut-treated explants, with *hairy2* experimental explants showing 4 in 4 pairs with differences, while control explants had only 1 in 4 pairs, and *meso1* experimental explants had only 4 in 5 pairs, while control explants were identical (n = 3). Interestingly, the differences are greater in explants cultured for 12h, compared to those cultured for 6h (Fig. 21 and 22, arrows and arrowheads). Together these results indicate that the lack of tension leads to fewer somites being formed (Fig. 15) and to a delay of the expression of *hairy2* and *meso1*, with this effect getting stronger the longer the explants are in contact with the drug (Fig. 16).

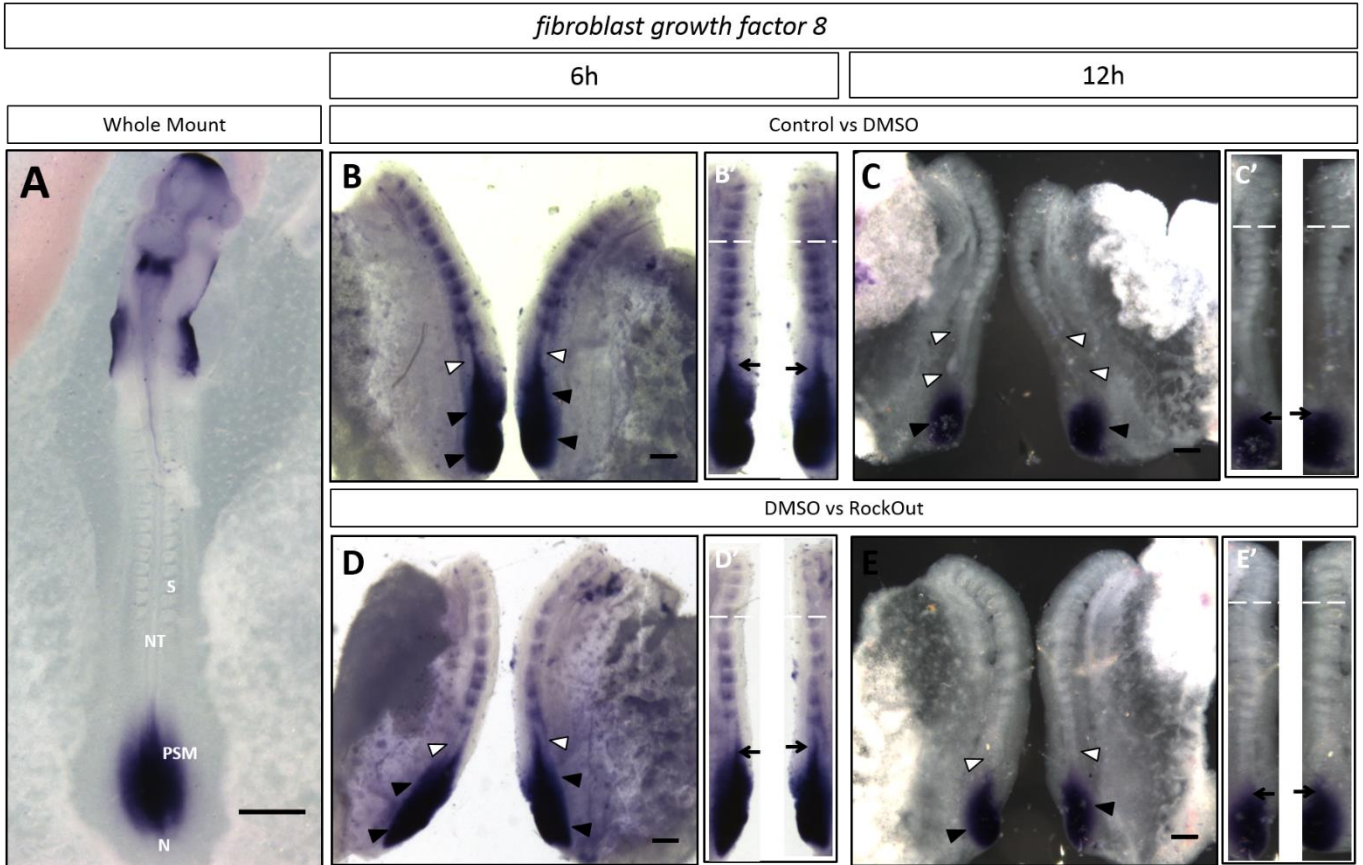


Figure 19 - *fgf8* expression pattern in explants cultured for 6h or 12h appears to reach slightly more anteriorly when tension is lacking, suggesting a delay in cellular differentiation. (A) *fgf8* expression in an intact nonmanipulated embryo for comparison. (B,B',C,C') *fgf8* expression in control pairs of explants, to rule out DMSO effects. (D,D',E,E') *fgf8* expression pattern in experimental pairs of explants, to assess RockOut effects. (B',C',D',E') Straightened paraxial mesoderms from B, C, D and E, respectively, to allow comparison of axial extension and position of the pattern. S – Somite, NT- Neural Tube, PSM – Presomitic Mesoderm, N – Node. White arrowheads indicate areas of the PSM voided of expression. Black arrowheads indicate areas of the PSM where expression is observable. Arrows indicate the anterior-most margin of expression in the PSM. Scale bar represents 500µm in A and 200µm in B, C, D and E.

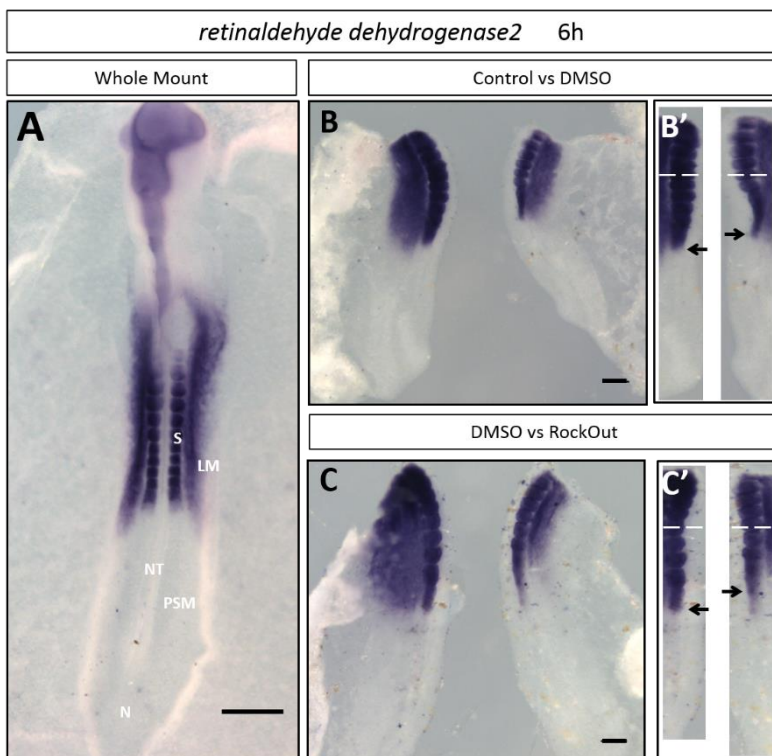


Figure 20 - *raldh2* expression pattern in explants cultured for 6h appears to be limited slightly more anteriorly when tension is lacking, suggesting a delay in cellular differentiation. (A) *raldh2* expression in an intact nonmanipulated embryo for comparison. (B,B') *raldh2* expression in a control pair of explants, to rule out DMSO effects. (C,C') *raldh2* expression pattern in an experimental pair of explants, to assess RO effects. (B',C') Straightened paraxial mesoderms from B and C, respectively, to allow comparison of axial extension and position of the pattern. S – Somite, NC- Notochord, PSM – Presomitic Mesoderm, LM- Lateral Mesoderm, N – Node. Arrows indicate the posterior-most margin of expression in the PSM. Scale bar represents 500µm in A and 200µm in B and C.

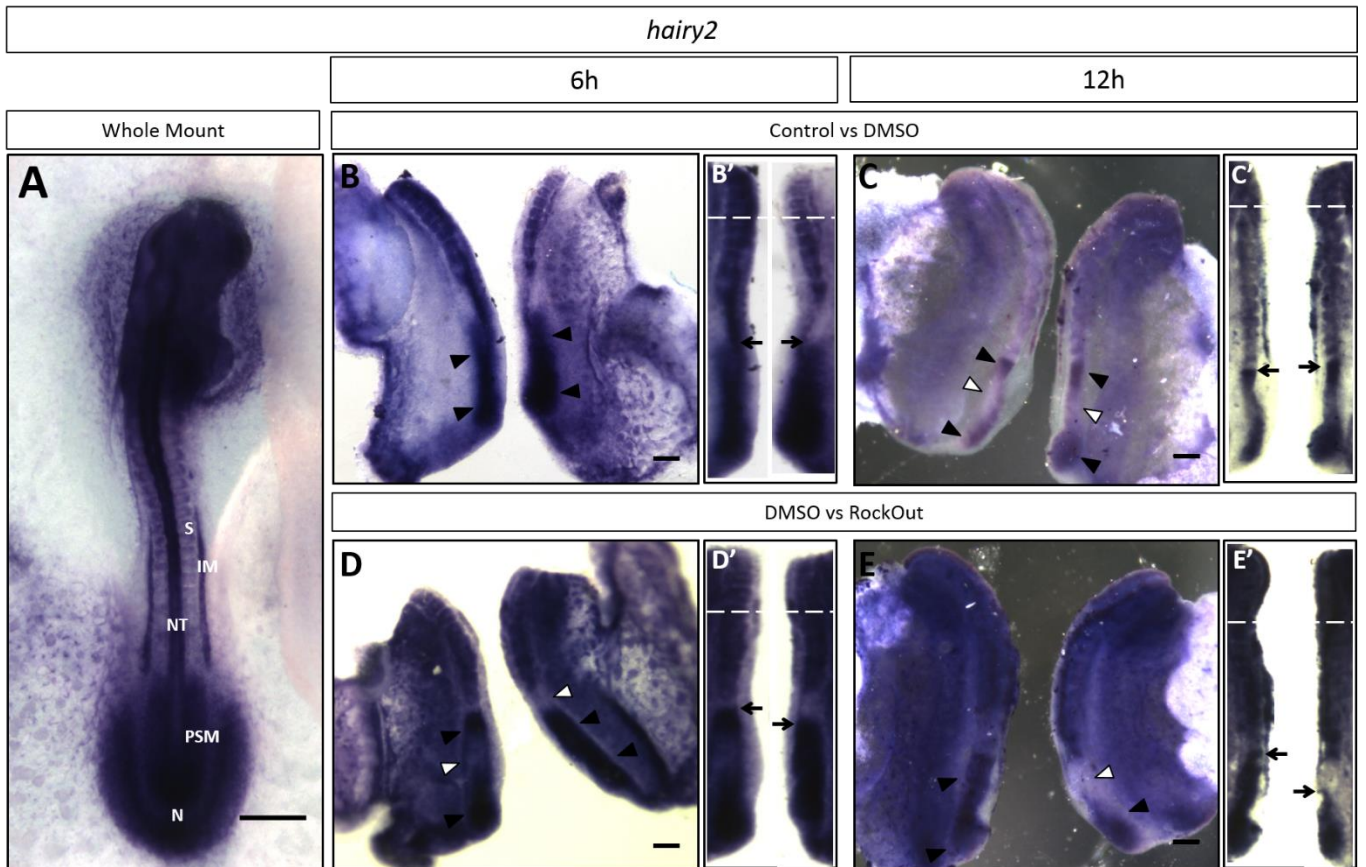


Figure 21 - *hairy2* expression pattern in explants cultured for 6h or 12h shows a difference in expression between experimental pairs, suggesting a delay in the cycle of expression. (A) *hairy2* expression in an intact nonmanipulated embryo for comparison. (B,B',C,C') *hairy2* expression in control pairs of explants, to rule out DMSO effects. (D,D',E,E') *hairy2* expression pattern in experimental pairs of explants, to assess RockOut effects. (B',C',D',E') Straightened paraxial mesoderms from B, C, D and E, respectively, to allow comparison of axial extension and position of the pattern. S – Somite, NT- Neural Tube, PSM – Presomitic Mesoderm, IM – Intermediate Mesoder, N – Node. White arrowheads indicate areas of the PSM without expression. Black arrowheads indicate areas of the PSM where expression is observable. Arrows indicate the anterior-most margin of expression in the PSM. Scale bar represents 500µm in A and 200µm in B,C, D and E.

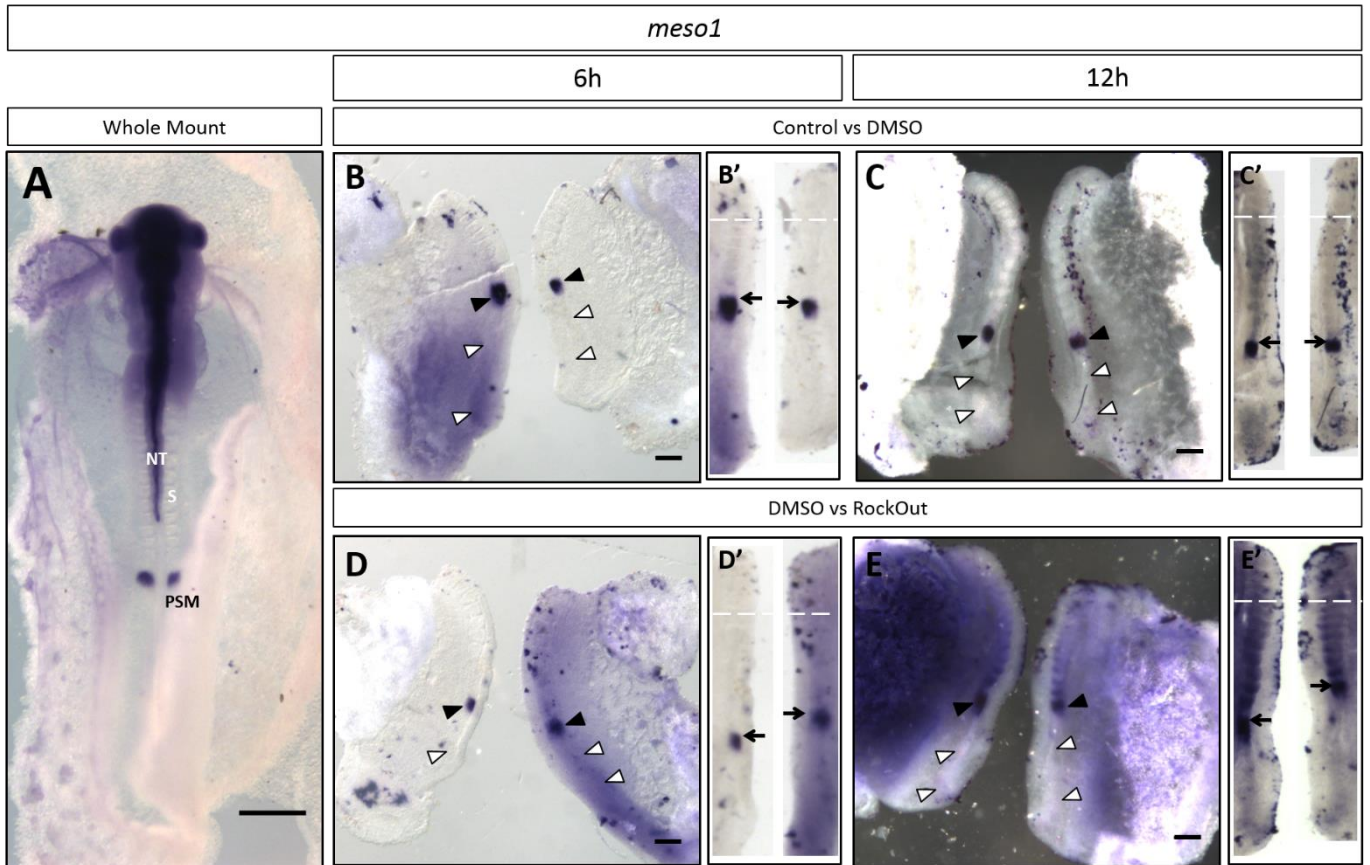


Figure 22 - *meso1* expression pattern in explants cultured for 6h or 12h shows a difference in expression between experimental pairs, suggesting a delay in the cycle of expression. (A) *meso1* expression in an intact nonmanipulated embryo for comparison. (B,B',C,C') *meso1* expression in control pairs of explants, to rule out DMSO effects. (D,D',E,E') *meso1* expression pattern in experimental pairs of explants, to assess RockOut effects. (B',C',D',E') Straightened paraxial mesoderms from B, C, D and E, respectively, to allow comparison of axial extension and position of the pattern. S – Somite, NT- Neural Tube, PSM – Presomitic Mesoderm. White arrowheads indicate areas of the PSM without expression. Black arrowheads indicate areas of the PSM where expression is observable. Arrows indicate the anterior-most margin of expression in the PSM. Scale bar represents 500 $\mu$ m in A and 200 $\mu$ m in B,C, D and E.

# Discussion

## The Development of Matrix Assembly

In recent years, several studies have related cellular and matrix tension with the regulation of developmental processes *in vivo* and with cellular differentiation *in vitro*<sup>66-68,75-81</sup>. In almost all of these experiments it is not made very clear where the matrix produced and what is its role in regulating these processes.

As mentioned before, several previous works have shown that fibronectin is important for somitogenesis, leading to the hypothesis that the gradient of fibronectin matrix, observed along the PSM, might provide essential physical cues (i.e. tension) for the regulation of somitogenesis. It was also proposed that this role is performed via a “paracrine-like” mechanism, where fibronectin produced by one tissue (e.g. ectoderm) is assembled by another (e.g. paraxial mesoderm). This proposal got further support from our work, as will be detailed below.

To understand if this proposed role for the fibronectin matrix is plausible, we decided to first examine how the matrix is formed, where it comes from, and how its development correlates with the processes necessary for paraxial mesoderm formation and somitogenesis. At the earliest stages of *in ovo* development (HH1-HH4) we found that *fn1* is expressed in a punctuated pattern. This *fn1* expression pattern is reminiscent of the topological organization of the so called hypoblast islands which form when cells delaminate from the epiblast in groups to form the underlying primary hypoblast (see Stern & Downs, 2012). However, those are reported for slightly earlier stages (stage X-XII), which we are not sure to have obtained, as there is some variability in the first developmental stage *in ovo*. It is thus essential to section the hybridized embryos, and perform other hybridizations for early hypoblast markers, to be able to evaluate the exact nature of these *fn1* expressing patches. At the same time, it appears that *itga5* is being expressed by the cells that give rise to the groove that will become the primitive streak, suggesting a higher assembly level of the FN matrix around this groove, which was indeed observed at stage HH4.

The FN matrix assembly pattern we observe is suggestive of a role of fibronectin in the migration of the gastrulating cells through the primitive streak and the node. This matrix is more clearly observable from the ventral side of the embryo, suggesting that the matrix is also more assembled there. We therefore propose that gastrulating cells use this newly assembled matrix as a scaffold to force their way in-between the already formed epiblast and hypoblast to originate the new embryonic tissues, endoderm and mesoderm.

From stage HH4 onwards the embryo goes through the gastrulation process as the node migrates caudally along the primitive streak. This leads to a progressive change in *fn1* and *itga5* expression. *fn1* starts being expressed, mostly, in the non-neural ectoderm and *itga5* expression comes on in the forming mesoderm. Up to stage HH8 the node has yet to reach the most caudal region of the embryo, and therefore we can still see a transitioning pattern of expression, from “pre-gastrulation” to “post-gastrulation”, probably indicative of a progressive alteration of the role of both genes between these two embryonic events/stages. From stage HH7 onwards the embryo also starts to form its heart, whose primordia shows some expression of *fn1*.

To confirm that after this change of roles the expression patterns were still indicative of the pattern of FN matrix assembly, we again performed immunofluorescence labeling for FN, this time at a stage HH8 embryo, where head formation, heart development, gastrulation, axial elongation and somitogenesis are well under way. Again we saw that the complexity of matrix assembly is intimately correlated with the levels of *fn1* expression, and that several places that show high assembly of the FN matrix also show high expression of *itga5*, such as the paraxial mesoderm. However, other regions, like the head and forming heart, show a very high assembly level of FN matrix, with great complexity, but low or no expression of *itga5*. This indicates that FN matrix is mostly assembled by other integrin dimers and/or other receptors in several tissues<sup>62,73</sup>, at least in these stages.

These results demonstrate that an antero-posterior gradient of FN matrix complexity exists in the chick embryo as early as stage HH4. Previous studies have shown that such a gradient exists in the paraxial mesoderm of HH12 embryos<sup>64</sup> and here we provide evidence to suggest that a gradient of FN matrix complexity exists from the earliest stages of development, and that this gradient correlates with the progression of somitogenesis. Interestingly, one of the most notable results is that from the inception of the paraxial mesoderm there is expression of *fn1* around it and high assembly of FN matrix in this tissue. However, there is no expression of *fn1* in this tissue, but there is of *itga5*. These results add very strong support to the proposed “paracrine-like” effect of FN on somitogenesis, at least throughout the early stages of embryonic development.

We need to also mention that FN matrix and Integrin  $\alpha5\beta1$  are present during gastrulation, and may play a role. Some studies have shown that tension and PCP signaling are important for gastrulation<sup>67,83</sup>. Whether FN and Integrin  $\alpha5\beta1$  also play a role in physical signaling during that process remains to be tested.

## The complicated relationship between tension and matrix

The proposal that the FN matrix gradient might be responsible for a physical signaling that cooperates in the regulation of the somitogenic process seems a very complicated hypothesis to test, due to the number of factors being influenced by a single variable changing. However, we can infer a somewhat strong conclusion by having several experiments all leading down the same logical path.

The first clues supporting this hypothesis have already been mentioned. The fact that the ectoderm shows a gradient of *fn1* expression overlappable with the gradient of matrix assembly seen around the PSM<sup>55,64</sup>, that without ectoderm and the FN matrix somitogenesis is interrupted<sup>53,55</sup>, but the addition of either is able to restore it, and that addition of FN to isolated PSMs after removal of their endogenous matrix can partially rescue somite formation all point to the possibility of a gradient of tension being produced by the FN matrix<sup>55</sup>.

Now we have further demonstrated that this gradient of expression and matrix assembly is actually a phenomenon that accompanies somitogenesis from the very beginning. However, there is still a lack of proof that any form of actual tension is indeed involved in the process of somitogenesis. To test its presence we decided to culture embryo explants with a Rho Kinase (ROCK) inhibiting drug, which results in an inhibition of non-muscle myosin II phosphorylation and, therefore, in an inability of the cell to exert force on the extracellular matrix.

Our first results from these explants indicated that a lack of tension leads to a delay in somitogenesis. To try and understand how the lack of tension affects the matrix and somite development we performed immunofluorescence assays against, FN, LN and N-Cadherin.

When treated with RockOut, explants show a strongly perturbed FN matrix, with the complex fibrillar form being replaced by patches of semi-extended and globular forms, and somites appearing to be less surrounded by FN matrix. These results could indicate that there is simply less production of FN. However, the *fn1* expression pattern is not significantly affected by culture with RockOut. Thus we hypothesize that the globular aggregate that we see are produced by the embryo and that they accumulate due to an impairment of FN matrix assembly. This also leads to an destabilization of the formed clefts, in agreement with FN's reported role in their maintenance<sup>56,60,70,55</sup>, and thus potentially explaining the high number of fused somites found.

Epithelialization seems to be more affected after 6h of culture than after 12h. However, even at 12h culture we see a slight effect on epithelialization, since controls seem to have a better defined somitocoel than experimental somites. This suggests that tension and/or proper matrix assembly is required for a correct epithelialization of the somite.

Curiously, the LN matrix seems to be affected by the lack of tension. Because Laminin trimers should not need extension, like FN molecules, to be able to form a firmly assembled matrix, since their binding sites are already all exposed, it seems logical that tension and receptor binding would be less essential for LN matrix assembly. Although the lack of tension seems to have little effect on LN matrix, it seems that there might be an increase of the amount of matrix surrounding the somites at 6h culture, and only a very slight increase in the 12h. This could be due to an attempt of the tissue to maintain its correct epithelialization, compensating

the partial loss of the FN matrix, by increasing the density of its LN matrix. This might explain why LN matrix seems denser the more the epithelialization is affected, but seems to decrease when it recovers. It would be interesting to determine whether the expression of laminin genes are upregulated in the explants cultured in RockOut for 6 hours.

## Does tension affect patterning?

The question of whether an alteration on the physical information received by a tissue could affect the genetic regulation of that tissue is a quite pertinent one. If physical cues can alter the migration path of a cell, or its differentiation state, obviously some genetic regulation must be behind these effects.

To test how genetic regulation of somitogenesis is affected by the loss of tension we performed cultures of bisected explants, as described above. This technique allows us to compare how genetic regulation is affected in the same tissue, of the same embryo, at the same time, but in different conditions. To assess this we performed *in situ hybridization* on these explants for genes that are known to play different, but indispensable, roles in somitogenesis.

We did not detect any significant alterations in the expression patterns of *fn1* and *itga5*. However, these observations should not be considered final since *in situ* hybridization is not ideal for assessing changes in expression levels. To properly test whether or not there is a change in expression levels after 12h culture, other methods will have to be use, like qPCR.

After that we examined the response of the “wavefront” genes to the lack of tension. The “wavefront”, as was mentioned before, is determined by opposing gradients of retinoic acid, decreasing from rostral to caudal, and *Fgf8*, decreasing from caudal to rostral<sup>30,84-86</sup>. The region of overlap of these gradients determines the axial position in which paraxial mesodermal cells become determined to form somites<sup>36</sup>. We found that the expression patterns of these genes are slightly influenced by the lack of tension. There appears to be a slight reduction of the posterior extension of *raldh2* expression pattern, which could indicate that cells are becoming determined later than in the control. Supporting this hypothesis is the observation that *fgf8* expression extends more rostrally, both at 6h and 12h, again suggesting that lack of tension delays the determination of PSM cells.

Lastly, we performed a new set of explant cultures to test the influence of lack of tension in the expression of two cycling genes, *hairy2* and *meso1*. Our experiment shows us that lack of tension strongly affects their mRNA expression pattern indicating that lack of tension leads to a reduction of the periodicity of the “embryonic clock”. To further support these results RockOut-treated explants form less somites than control explants (DMSO and Normal Chicken Medium explants). Although DMSO does indeed have some effect on the number of somites formed, its effects are very slight, and could be unspecific, being just the effect of a stressant/toxin. Immunofluorescence analysis did not show any significative effect of DMSO, suggesting that DMSO is having a minor effect on somitogenesis. Furthermore, not only did RockOut exacerbate all effects DMSO had, it also provoked several other effects not produced by DMSO. Therefore, this work also allows us to show that DMSO at the concentration used does not significantly

affect somitogenesis and thus is a good control for RockOut, removing the need for additional controls.

Taken all together, these results lead us to propose that from the start of somitogenesis the FN matrix is responsible for creating a gradient of physical signaling (e.g. tension) along the paraxial mesoderm, which appears to participate in the regulation of cell determination and cyclic gene expression periodicity. As for Integrin  $\alpha 5\beta 1$ , it probably serves a double purpose. First it acts as an assembly receptor of the FN matrix<sup>63,70-74</sup>, determining, in cooperation with FN production levels (and possibly other receptors), the layout of the gradient. After that, FN-binding Integrins will constitute an “outside-in” signaling pathway, and Integrin  $\alpha 5\beta 1$  will signal, possibly through pFAK<sup>39,70</sup>, the state of the matrix.

Lack of cellular tension leads to a smaller capability of extension of the FN molecules, which will lead to less, or a slower, assembly of the FN matrix. Less assembly of FN matrix will result in a looser, less tense (and therefore more bendable) matrix, which will affect Integrin-FN ligation. This results in less pFAK (or other) signaling, which, probably in cooperation with Notch signaling<sup>89</sup>, will tell the cell that it is still in a more posterior axial level, and should remain undetermined. However, if this cell has already received information that it is in a more anterior axial level (through retinoic acid levels, for instances), it appears that the lack of Integrin signaling results in a delay of cyclic gene expression. This delay will give the cells more time to produce matrix, and then receive the correct physical signaling, before they finish their differentiation and compact to form the new somite.

This signaling probably also happens in cooperation with the Notch signaling pathway, as previously suggested<sup>87,70</sup>. However, more work needs to be done to fully elucidate the role of tension in somitogenesis, e.g. how it interacts with Notch-signaling, if it affects the differentiation process, and whether it influences other pathways implicated in somitogenesis, such as Shh, Wnt, Fgf<sup>88</sup>.

To summarize, it would appear that tension acts like a “final checkpoint” for the processes happening during PSM determination, to make sure that all signaling pathways are synchronous before a somite is produced. If not, it is possible that this signal leads to changes in gene expression that allows the paraxial mesoderm a little more time to produce the matrix it needs to support the formation of a new somite.

# Bibliography

1. Pérez-Pomares, J.M. & Muñoz-Chápuli, R. Epithelial-mesenchymal transitions: a mesodermal cell strategy for evolutive innovation in Metazoans. *Anat. Rec.* **268**, 343–51 (2002).
2. Psychoyos, D. & Stern, C.D. Restoration of the organizer after radical ablation of Hensen's node and the anterior primitive streak in the chick embryo. *Development* **122**, 3263–3273 (1996).
3. Wang, Y. & Steinbeisser, H. Molecular basis of morphogenesis during vertebrate gastrulation. *Cell. Mol. Life Sci.* **66**, 2263–73 (2009).
4. Solnica-Krezel, L. & Sepich, D.S. Gastrulation: making and shaping germ layers. *Annu. Rev. Cell Dev. Biol.* **28**, 687–717 (2012).
5. Christ, B., Huang, R. & Scaal, M. Formation and differentiation of the avian sclerotome. *Anat. Embryol.* **208**, 333–50 (2004).
6. Scaal, M. & Christ, B. Formation and differentiation of the avian dermomyotome. *Anat. Embryol.* **208**, 411–24 (2004).
7. Noden, D.M. Interactions and fates of avian craniofacial mesenchyme. *Development* **103 Suppl**, 121–140 (1988).
8. Couly, G.F., Coltey, P.M. & Le Douarin, N.M. The developmental fate of the cephalic mesoderm in quail-chick chimeras. *Development* **114**, 1–15 (1992).
9. Gomez, C. *et al.* Control of segment number in vertebrate embryos. *Nature* **454**, 335–9 (2008).
10. Martins, G.G. *et al.* Dynamic 3D cell rearrangements guided by a fibronectin matrix underlie somitogenesis. *PLoS One* **4**, e7429 (2009).
11. Bellairs, R. The mechanism of somite segmentation in the chick embryo. *J. Embryol. Exp. Morphol.* **51**, 227–43 (1979).
12. Christ, B. & Ordahl, C. P. Early stages of chick somite development. *Anat. Embryol.* **191**, 381–96 (1995).
13. Kalchauer, C. & Ben-Yair, R. Cell rearrangements during development of the somite and its derivatives. *Curr. Opin. Genet. Dev.* **15**, 371–80 (2005).
14. Ebner V. von 1888. Urwirbel und Neugliederung der Wirbelsäule. *Sitzungsber Akad Wiss Wien III/97*:194–206.
15. Christ B. Die Entwicklung der Körperwandmetamerie, experimentelle Untersuchungen an Hühnerembryonen. Habilitationsschrift, Ruhr-Universität Bochum (1975).
16. Cooke, J. & Zeeman, E. C. A clock and wavefront model for control of the number of repeated structures during animal morphogenesis. *J. Theor. Biol.* **58**, 455–76 (1976).

17. Palmeirim, I., Henrique, D., Ish-Horowicz, D. & Pourquié, O. Avian *hairy* gene expression identifies a molecular clock linked to vertebrate segmentation and somitogenesis. *Cell* **91**, 639–48 (1997).
18. Conlon, R.A., Reaume, A.G. & Rossant, J. Notch1 is required for the coordinate segmentation of somites. *Development* **121**, 1533–45 (1995).
19. Bettenhausen, B., Hrabě de Angelis, M., Simon, D., Guénet, J.L. & Gossler, A. Transient and restricted expression during mouse embryogenesis of *Dll1*, a murine gene closely related to *Drosophila* Delta. *Development* **121**, 2407–2418 (1995).
20. Dunwoodie, S.L., Henrique, D., Harrison, S.M. & Beddington, R.S. Mouse *Dll3*: a novel divergent Delta gene which may complement the function of other Delta homologues during early pattern formation in the mouse embryo. *Development* **124**, 3065–3076 (1997).
21. Feder, J.N., Jan, L.Y. & Jan, Y.N. A rat gene with sequence homology to the *Drosophila* gene *hairy* is rapidly induced by growth factors known to influence neuronal differentiation. *Mol. Cell. Biol.* **13**, 105–113 (1993).
22. Jouve, C. *et al.* Notch signalling is required for cyclic expression of the hairy-like gene *HES1* in the presomitic mesoderm. *Development* **127**, 1421–9 (2000).
23. Leimeister, C. *et al.* Oscillating expression of *c-Hey2* in the presomitic mesoderm suggests that the segmentation clock may use combinatorial signaling through multiple interacting bHLH factors. *Dev. Biol.* **227**, 91–103 (2000).
24. Bessho, Y. *et al.* Dynamic expression and essential functions of *Hes7* in somite segmentation. *Genes Dev.* **15**, 2642–7 (2001).
25. Holley, S.A., Geisler, R. & Nüsslein-Volhard, C. Control of *her1* expression during zebrafish somitogenesis by a Delta- dependent oscillator and an independent wave-front activity. *Genes Dev.* **14**, 1678–1690 (2000).
26. Oates, A.C. & Ho, R.K. Hairy/E(spl)-related (Her) genes are central components of the segmentation oscillator and display redundancy with the Delta/Notch signaling pathway in the formation of anterior segmental boundaries in the zebrafish. *Development* **129**, 2929–2946 (2002).
27. Buchberger, A., Seidl, K., Klein, C., Eberhardt, H. & Arnold, H.H. *cMeso-1*, a novel bHLH transcription factor, is involved in somite formation in chicken embryos. *Dev. Biol.* **199**, 201–15 (1998).
28. Saga, Y. *et al.* *MesP1*: a novel basic helix-loop-helix protein expressed in the nascent mesodermal cells during mouse gastrulation. *Development* **122**, 2769–2778 (1996).
29. Saga, Y., Hata, N., Koseki, H. & Taketo, M.M. *Mesp2*: a novel mouse gene expressed in the presegmented mesoderm and essential for segmentation initiation. *Genes Dev.* **11**, 1827–1839 (1997).

30. Dubrulle, J., McGrew, M.J. & Pourquié, O. FGF signaling controls somite boundary position and regulates segmentation clock control of spatiotemporal Hox gene activation. *Cell* **106**, 219-232 (2001).
31. Yamaguchi, T.P., Conlon, R.A. & Rossant, J. Expression of the fibroblast growth factor receptor FGFR-1/flg during gastrulation and segmentation in the mouse embryo. *Dev. Biol.* **152**, 75-88 (1992).
32. Swindell, E.C. *et al.* Complementary domains of retinoic acid production and degradation in the early chick embryo. *Dev. Biol.* **216**, 282–96 (1999).
33. Sato, Y., Yasuda, K. & Takahashi, Y. Morphological boundary forms by a novel inductive event mediated by Lunatic fringe and Notch during somitic segmentation. *Development* **129**, 3633–44 (2002).
34. Hirata, H. *et al.* Oscillatory expression of the bHLH factor Hes1 regulated by a negative feedback loop. *Science* **298**, 840–3 (2002).
35. Nakajima, Y., Morimoto, M., Takahashi, Y., Koseki, H. & Saga, Y. Identification of Epha4 enhancer required for segmental expression and the regulation by Mesp2. *Development* **133**, 2517–25 (2006).
36. Diez del Corral, R. *et al.* Opposing FGF and retinoid pathways control ventral neural pattern, neuronal differentiation, and segmentation during body axis extension. *Neuron* **40**, 65–79 (2003).
37. Niwa, Y. *et al.* Different types of oscillations in notch and Fgf signaling regulate the spatiotemporal periodicity of somitogenesis. *Genes Dev.* **25**, 1115-1120 (2011).
38. Duband, J. L. *et al.* Adhesion molecules during somitogenesis in the avian embryo. *J. Cell Biol.* **104**, 1361–74 (1987).
39. Henry, C.A. *et al.* Roles for zebrafish focal adhesion kinase in notochord and somite morphogenesis. *Dev. Biol.* **240**, 474–87 (2001).
40. Burgess, R., Cserjesi, P., Ligon, K. & Olson, E. Paraxis: a basic helix-loop-helix protein expressed in paraxial mesoderm and developing somites. *Dev. Biol.* (1995).
41. Barnes, G.L., Alexander, P.G., Hsu, C.W., Mariani, B.D. & Tuan, R.S. Cloning and characterization of chicken Paraxis: a regulator of paraxial mesoderm development and somite formation. *Dev. Biol.* **189**, 95–111 (1997).
42. Johnson, J. *et al.* The anterior/posterior polarity of somites is disrupted in paraxis-deficient mice. *Dev. Biol.* **229**, 176–87 (2001).
43. Rowton, M. *et al.* Regulation of mesenchymal-to-epithelial transition by PARAXIS during somitogenesis. *Dev. Dyn.* **242**, 1332-1344 (2013).
44. Ebensperger, C. *et al.* Pax-1, a regulator of sclerotome development is induced by notochord and floor plate signals in avian embryos. *Anat. Embryol.* **191**, 297–310 (1995).
45. Borycki, A. G., Mendham, L. & Emerson, C. P. Control of somite patterning by Sonic hedgehog and its downstream signal response genes. *Development* **125**, 777–90 (1998).

46. Borycki, A., Brown, A. M. & Emerson, C. P. Shh and Wnt signaling pathways converge to control Gli gene activation in avian somites. *Development* **127**, 2075–87 (2000).
47. Resende, T. P. *et al.* Sonic hedgehog in temporal control of somite formation. *Proc. Natl. Acad. Sci. U.S.A.* **107**, 12907–12 (2010).
48. Aulehla, A. *et al.* Wnt3a plays a major role in the segmentation clock controlling somitogenesis. *Dev. Cell* **4**, 395–406 (2003).
49. Schmidt, C. *et al.* Wnt 6 regulates the epithelialisation process of the segmental plate mesoderm leading to somite formation. *Dev. Biol.* **271**, 198–209 (2004).
50. Linker, C. *et al.*  $\beta$ -Catenin-dependent Wnt signalling controls the epithelial organisation of somites through the activation of paraxis. *Development* **132**, 3895–905 (2005).
51. Dzamba, B. J., Jakab, K. R., Marsden, M., Schwartz, M.A & DeSimone, D.W. Cadherin adhesion, tissue tension, and noncanonical Wnt signaling regulate fibronectin matrix organization. *Dev. Cell* **16**, 421–32 (2009).
52. Neijts, R., Simmini, S., Giuliani, F., Rooijen, C. van & Deschamps, J. Region-specific regulation of posterior axial elongation during vertebrate embryogenesis. *Dev. Dyn.* **243**, 88–98 (2014).
53. Palmeirim, I., Dubrulle, J., Henrique, D., Ish-Horowicz, D. & Pourquié, O. Uncoupling segmentation and somitogenesis in the chick presomitic mesoderm. *Dev. Genet.* **23**, 77–85 (1998).
54. Correia, K.M. & Conlon, R.A. Surface ectoderm is necessary for the morphogenesis of somites. *Mech. Dev.* **91**, 19–30 (2000).
55. Rifes, P. *et al.* Redefining the role of ectoderm in somitogenesis: a player in the formation of the fibronectin matrix of presomitic mesoderm. *Development* **134**, 3155–65 (2007).
56. Lash, J. W., Seitz, a W., Cheney, C. M. & Ostrovsky, D. On the role of fibronectin during the compaction stage of somitogenesis in the chick embryo. *J. Exp. Zool.* **232**, 197–206 (1984).
57. Muschler, J.L. & Horwitz, A.F. Down-regulation of the chicken alpha 5 beta 1 integrin fibronectin receptor during development. *Development* **113**, 327–37 (1991).
58. George, E.L., Georges-Labouesse, E.N., Patel-King, R.S., Rayburn, H. & Hynes, R.O. Defects in mesoderm, neural tube and vascular development in mouse embryos lacking fibronectin. *Development* **119**, 1079–91 (1993).
59. Yang, J. T., Rayburn, H. & Hynes, R. O. Embryonic mesodermal defects in alpha 5 integrin-deficient mice. *Development* **119**, 1093–105 (1993).
60. Georges-Labouesse, E. N., George, E. L., Rayburn, H. & Hynes, R. O. Mesodermal development in mouse embryos mutant for fibronectin. *Dev. Dyn.* **207**, 145–56 (1996).
61. Goh, K.L., Yang, J.T. & Hynes, R.O. Mesodermal defects and cranial neural crest apoptosis in alpha5 integrin-null embryos. *Development* **124**, 4309–19 (1997).

62. Yang, J. T. *et al.* Overlapping and independent functions of fibronectin receptor integrins in early mesodermal development. *Dev. Biol.* **215**, 264–77 (1999).
63. Mao, Y. & Schwarzbauer, J.E. Stimulatory effects of a three-dimensional microenvironment on cell-mediated fibronectin fibrillogenesis. *J. Cell Sci.* **118**, 4427–36 (2005).
64. Rifes, P. & Thorsteinsdóttir, S. Extracellular matrix assembly and 3D organization during paraxial mesoderm development in the chick embryo. *Dev. Biol.* **368**, 370–81 (2012).
65. Hiramatsu, R. *et al.* External mechanical cues trigger the establishment of the anterior-posterior axis in early mouse embryos. *Dev. Cell* **27**, 131–44 (2013).
66. Mammoto, T., Mammoto, A. & Ingber, D.E. Mechanobiology and developmental control. *Annu. Rev. Cell Dev. Biol.* **29**, 27-61 (2013).
67. Hara, Y. *et al.* Directional migration of leading-edge mesoderm generates physical forces: Implication in *Xenopus* notochord formation during gastrulation. *Dev. Biol.* **382**, 482-495 (2013).
68. Piccolo, S. Mechanics in the embryo. *Nature* **504**, 223-225 (2013).
69. Hamburger, V. & Hamilton, H.L. A series of normal stages in the development of the chick embryo. 1951. *Dev. Dyn.* **195**, 231-272 (1992).
70. Koshida, S. *et al.* Integrin $\alpha$ 5-dependent fibronectin accumulation for maintenance of somite boundaries in zebrafish embryos. *Dev. Cell* **8**, 587–98 (2005).
71. Larsen, M., Artym, V.V., Green, J.A. & Yamada, K.M. The matrix reorganized: extracellular matrix remodeling and integrin signaling. *Curr. Opin. Cell Biol.* **18**, 463–71 (2006).
72. Leiss, M., Beckmann, K., Girós, A., Costell, M. & Fässler, R. The role of integrin binding sites in fibronectin matrix assembly in vivo. *Curr. Opin. Cell Biol.* **20**, 502–7 (2008).
73. Singh, P., Carraher, C. & Schwarzbauer, J.E. Assembly of fibronectin extracellular matrix. *Annu. Rev. Cell Dev. Biol.* **26**, 397-419 (2010).
74. Girós, A., Grgur, K., Gossler, A. & Costell, M.  $\alpha$ 5 $\beta$ 1 Integrin-mediated adhesion to fibronectin is required for axis elongation and somitogenesis in mice. *PLoS One* **6**, e22002 (2011).
75. Walker, J.L., Fournier, A.K. & Assoian, R.K. Regulation of growth factor signaling and cell cycle progression by cell adhesion and adhesion-dependent changes in cellular tension. *Cytokine Growth Factor Rev.* **16**, 395–405 (2005).
76. Assoian, R.K. & Klein, E.A. Growth control by intracellular tension and extracellular stiffness. *Trends Cell Biol.* **18**, 347–52 (2008).

77. Daley, W.P., Gulfo, K.M., Sequeira, S.J. & Larsen, M. Identification of a mechanochemical checkpoint and negative feedback loop regulating branching morphogenesis. *Dev. Biol.* **336**, 169–82 (2009).
78. Campinho, P. *et al.* Tension-oriented cell divisions limit anisotropic tissue tension in epithelial spreading during zebrafish epiboly. *Nat. Cell Biol.* **15**, 1405–1414 (2013).
79. Daley, W.P. & Yamada, K.M. ECM-modulated cellular dynamics as a driving force for tissue morphogenesis. *Curr. Opin. Gen. Dev.* **23**, 408-414 (2013).
80. Hiramatsu, R. *et al.* External mechanical cues trigger the establishment of the anterior-posterior axis in early mouse embryos. *Dev. Cell* **27**, 131–44 (2013).
81. Menko, A.S., Bleaken, B.M. & Walker, J.L. Regional-specific alterations in cell-cell junctions, cytoskeletal networks and myosin-mediated mechanical cues coordinate collectivity of movement of epithelial cells in response to injury. *Exp. Cell Res.* **322**, 133-148 (2014).
82. Stern, C.D. & Downs, K.M. The hypoblast (visceral endoderm): an evo-devo perspective. *Development* **139**, 1059–69 (2012).
83. Dohn, M.R., Mundell, N.A., Sawyer, L.M., Dunlap, J.A. & Jessen, J.R. Planar cell polarity proteins differentially regulate extracellular matrix organization and assembly during zebra fish gastrulation. *Dev. Biol.* 1-13 (2013).
84. Maden, M., Graham, A., Zile, M. & Gale, E. Abnormalities of somite development in the absence of retinoic acid. *Int. J. Dev. Biol.* **44**, 151-159 (2000).
85. Pourquié, O. Vertebrate somitogenesis: a novel paradigm for animal segmentation? *Int. J. Dev. Biol.* **47**, 597–603 (2003).
86. Freitas, C., Rodrigues, S., Saúde, L. & Palmeirim, I. Running after the clock. *Int. J. Dev. Biol.* **49**, 317–24 (2005).
87. Jülich, D., Geisler, R. & Holley, S.A. Integrin $\alpha$ 5 and delta/notch signaling have complementary spatiotemporal requirements during zebrafish somitogenesis. *Dev. Cell* **8**, 575–86 (2005).
88. Bénazéraf, B. & Pourquié, O. Formation and segmentation of the vertebrate body axis. *Annu. Rev. Cell Dev. Biol.* **29**, 1–26 (2013).

# Supplementary protocols

## Extended probe production protocol

Plasmids were first transfected into 50µl of DHα5<sup>TM</sup> *E. coli* (Invitrogen #18265017) competent cells. 1µL of plasmid (1 to 10 ng, diluted in TE) was used in the transfection. After transfection the bacteria were incubated for 30 minutes on ice, then heat-shocked at 42°C for 20 seconds, and quickly placed back on ice for 2 minutes. 950µL of plain LB medium [10mg/mL of Casein Peptone (Merck #102239) 5mg/mL of Yeast Extract (Merck #103753) 86mM of NaCl] were added, and the bacteria were incubated for 1h, at 37°C, shaking at 225rpm. After that, 100µL of each vial were plated in solid selection medium [LB with 100µg/mL of Ampicillin (Sigma #A0166) and 1.5% Agarose (Frlabo #604001)] that were incubated inverted, overnight (O/N), at 37°C.

The next day four colonies from each plate were selected and transferred to four 15mL Falcon tubes, each with 4mL of LB selection medium (100µg/mL Ampicillin), and incubated at 37°C and 300rpm for 8 hours.

To determine which tube contained the highest amount of plasmid-containing cells, we performed a Mini Prep. 1mL of each culture tube was collected, vortexed, and its pellet resuspended in 100µL of TE containing RNase (10µg/mL, Nzytech #MB18701). Cells were then lysed by adding 300µL of TENS (10mM of Tris-HCl pH7,5, 1mM EDTA, 0.1M NaOH and 0.5% SDS, Merck #113760), and the cellular contents were separated from the DNA by precipitating with 150µL of KAc at 3M, pH5,2, and after centrifugation the supernatant was transferred to a new tube, where the DNA was precipitated in 900µL of 100% EtOH. Finally, the dried pellet was resuspended in 50µL of TE [10mM Tris-HCl, (VWR #28808294) pH8, and 1mM EDTA (Sigma #E4884), pH8, in DEPC-treated (VWR #E174) water] and 1µL of the solution was run in a 1% agarose gel, with 4µL of sterile filtered water (Sigma #95284) and 1µL of 6x loading buffer (Promega #G190A), with 1µL of GreenSafe (Nzytech #MB13201) for 30-45 minutes, at 100 volts.

The culture tube that produced the clearest band was used to do a secondary culture, for 16h at 37°C, 300 rpm, by placing 500µL of the bacteria containing medium into an Erlenmeyer containing 100mL of liquid selection LB medium (with 100µg/mL of Ampicillin). After that period, DNA extraction was performed using the NucleoBond PC100 Midi Prep kit (Macherey-Nagel, #740573) using the standard protocol. At the end the pellet was dissolved in 30µL of TE, the concentration of the DNA measured in a NanoDrop<sup>TM</sup> 1000 (Thermo Scientific) spectrophotometer, and placed at -20°C for future use.

From that DNA, 10 $\mu$ g were removed and diluted in a 100 $\mu$ L solution, with 5-10U of the appropriate restriction enzyme and 10 $\mu$ L of each enzyme's buffer solution in sterile filtered water, to produce linearized template DNA for transcription. The digestion reaction took place at 37°C for 2h30m. After 2h of the digestion, 1 $\mu$ L of the solution was extracted, and run in a 1% agarose gel, for 30-45 minutes at 100-120 volts, as previously described.

After the digestion the DNA was precipitated in a 300 $\mu$ L DEPC water and 800 $\mu$ L isopropanol solution, for at least 2 hours (or O/N) at -20°C. After that it was centrifuged 3 times, for 20, 15 and 5 minutes, respectively, at 4°C, in the original solution, in 100% EtOH, and finally at 70% EtOH (diluted in DEPC-treated water), and the pellet was dried and dissolved in 30 $\mu$ L of TE. The DNA concentration was measured in a NanoDrop™ spectrophotometer, and saved at -20°C for future use.

From that volume, the corresponding to 1 $\mu$ g of template DNA was removed, and a transcription solution containing 2 $\mu$ L of 10x transcription buffer, the DNA, 2 $\mu$ L DIG/Fluorescein labelling mix (Roche #11277073910, Roche #11685619910, respectively), 1 $\mu$ L DTT (Promega #PROMP1171), 0,5 $\mu$ L of Rnasin (Promega #PROMN2111) and 1 $\mu$ L of appropriate RNA polymerase, diluted in sterile filtered water for a final volume of 20 $\mu$ L, was produced. The transcription reaction took place at 37°C, for 2h30. At the end of 2 hours 1 $\mu$ L of the solution was removed, and run in a 2% agarose gel, for 10-15 minutes at 100V as previously described, to check for correct transcription.

After the transcription reaction, 2.5 $\mu$ L of LiCl at 4M, 1 $\mu$ L of EDTA at 0.5M, pH8, and 75 $\mu$ L of 100% EtOH were used to precipitate the RNA for at least 2 hours (or O/N) at -20°C.

Finally the RNA was isolated by centrifuging at 13000 rpm for 45 minutes, at 4°C, then centrifuging 15 minutes, under the same conditions, in 200 $\mu$ L of 70% EtOH (diluted in DEPC-treated water), left to dry slightly, and finally diluted in 50 $\mu$ L of DEPC-treated water. The RNA concentration measured in a NanoDrop™ spectrophotometer. The RNA was then diluted in Hybridization Mix Hybmix, 50% Formamide, 195mM of NaCl, 19.5mM of Tri Sodium Citrate, 5mM of EDTA pH8, 0.05mg/mL of tRNA (Roche #10109495001), 0.2% Tween (Sigma #P1379), 5mg/mL of CHAPS (VWR #220201), and 0.1mg/mL of Heparin (Sigma #H6512), in DEPC (0.05%) - treated water to a final probe concentration of 1 $\mu$ g/mL, and stored at -20°C until use.